Thioflavin T: induced circular dichroism and density functional theory as promising approach in amyloid fibril assays
Aurica Precupas, Iulia Matei *
"Ilie Murgulescu" Institute of Physical Chemistry of the Romanian Academy, 202 Splaiul Independentei, 060021 Bucharest, Romania
* Correspondence: iulia.matei@yahoo.com; iuliamatei@icf.ro

Abstract

Amyloid research is oriented at present towards finding advanced methods that can provide viable diagnosis and treatment options. For this to be achieved, the fundamentals of protein aggregation into fibrils need to be clarified. Among spectroscopic techniques, UV-Vis and fluorescence are widely employed in amyloid assays. This review evaluates the potential of another spectroscopic method, induced circular dichroism (ICD), coupled with molecular modeling, specifically density functional theory (DFT), to provide accurate information on conformational changes of thioflavin T (ThT), an amyloid dye, upon binding to amyloid fibrils. We begin by recalling general aspects of the molecular rotor behaviour of ThT, which plays the critical role in chirality induction, and the basic principles of ICD. Then, we present an overview of literature works revealing chirality-inducing interactions of ThT, from early pioneering studies to notable recent contributions, pointing out remarkable achievements and ongoing challenges. We follow by addressing the progress made in computationally assessing ThT interactions, drawing attention to the unexplored potential of the ICD/DFT approach as amyloid diagnostic tool complementary to fluorescence. Through this review, we hope to encourage researchers to further document the capabilities of the ICD/DFT method, expanding the use of the ThT dye beyond its traditional fluorescence applications.

Keywords: thioflavin T; amyloid; protein; circular dichroism; density functional theory

Introduction

Amyloidosis is the general term for a wide range of protein-misfolding disorders in which insoluble amyloid fibrils accumulate in tissues and organs, disrupting their normal function. The three most common types of the disease are primary or immunoglobulin light chain (AL) amyloidosis, secondary or serum amyloid A (AA) amyloidosis and familial transthyretin (ATTR) amyloidosis. [1,2] Amyloid formation plays a significant role in the pathogenesis of multiple disorders including neurodegenerative diseases like Alzheimer's and Parkinson's, and type II diabetes. Definitive diagnosis of amyloidosis can only be made through tissue biopsy, one of the challenges being the identification of the amyloidogenic protein in order to provide disease-specific treatment aiming at symptoms management. Since no cure for amyloidosis is available at present, [3] early detection represents a top priority for health sciences.

The reason why few amyloid inhibitor compounds pass clinical trials, and none has yet been confirmed as effective treatment, is the insufficient comprehension of fibril formation and the limitations of the experimental methods used to quantify it. Current understanding indicates that amyloid formation is a multistep macromolecular self-assembly process caused by the inability of a protein to correctly fold into or to maintain its functionally active conformation. ^[4] In misfolded state, hydrophobic residues become solvent-exposed and thus prone to associate into aggregates, and further into fibrils. Protein aggregation is considered a kinetically controlled process that may lead to amyloid polymorphs, that is, multiple fibril conformations formed from a single polypeptide chain sequence. ^[5,6] The resulting heterogeneous, dynamic nature of these systems poses difficulties for routine structural studies. All native proteins have the generic ability to form fibrils in certain, at times non-physiological, conditions. This is why thermal treatment studies are essential for gaining insight into the factors that influence the aggregation behaviour. The thermal stability of proteins upon interaction with ligands that show potential as aggregation inhibitors has been one of the main research topics in our group during the past eight years. ^[7–14]

Both *ex vivo* amyloid detection in tissues and *in vitro* studies on fibril formation and growth rely on the use of optical assays based on staining with amyloid-specific dyes. They are fluorogenic probes whose emission intensity increases up to three orders of magnitude upon binding amyloids. Ideally, such probes only interact with fibrils, not with the native protein or other non-fibrillar constituents of the system. This specificity of amyloid dyes arises from recognizing the repetitive β -sheet structural motif that is common to all amyloids. [15]

Among amyloid-specific dyes, thioflavin T (ThT) is the most widely used due to the sensitivity of its spectral signature to microenvironmental properties that originates in its behaviour as molecular rotor. The reader is referred to excellent reviews that detail the molecular mechanisms of ThT binding to amyloid fibrils and offer comprehensive guidelines on conducting ThT amyloid assays. New ThT derivatives are constantly being developed, and their interaction with amyloids is investigated in view of their application for amyloidosis detection *in vitro* and/or *in vivo*, using advanced methods like positron emission tomography, as well as in the context of elucidating the pathogenesis of amyloidosis and developing efficient inhibitors. As an example, Pittsburgh compound B was the first ThT derivative successfully used *in vivo* for the detection and quantitative evaluation of amyloid plaques in Alzheimer's patients. Advanced fluorescence techniques are also emerging, with ThT being used as molecular probe to explore their capabilities in the amyloid field. Advanced

The use of spectral probes to study interactions in biological and biocompatible systems is well established and requires knowledge of the link between the spectral signature of the probe and the processes taking place. Relevant contributions in recent years from our research group and collaborators are exemplified in several papers. [43-51] As detailed in invited perspective [52] and review [53] articles, special emphasis has been paid to chirality inducing interactions as a handy means of collecting structural information at molecular scale. To this end, we proposed a concerted approach pairing induced circular dichroism (ICD) experimental measurements with (time-dependent) density functional theory (TD)DFT calculations, and successfully applied it to identify the species and conformation of protein-bound ligands belonging to the polyphenol [54-56] and coumarin^[57,58] classes, both with demonstrated amyloid inhibitor activity. [59-61] The method can be applied to achiral ligands that bear one or more torsional degrees of freedom which become hindered upon binding to a macromolecular host. The origin of the induced chirality is the conformational adaptation of the ligand to the steric requirements of the binding pocket, a so-called "chiral twist" in which intramolecular rotation is followed by entrapment of a twisted, thus chiral, rigid conformer. The sensitivity of ICD to subtle structural alterations at the binding site makes it a very desirable method for studying binding events associated with ligand and/or protein conformational changes. Furthermore, the ICD/DFT procedure has been established as a reliable alternative to traditional high-resolution techniques like solution NMR spectroscopy and X-ray crystallography, whose application to protein-bound ligands and, by extension, to amyloid-bound ligands is by far more strenuous.

As unravelled by Dzwolak and Pecul,^[62] the entrapment of ThT by amyloid fibrils leads not only to highly fluorescent conformers, but also to optically active conformers. This is due to the molecular rotor behaviour of ThT, which has been extensively exploited in fluorescence but is equally essential for ICD as it favours the "chiral twist" chirality-induction mechanism. In addition, the monomeric^[62] and dimeric^[63] forms of ThT have very distinct ICD spectral signatures, each with magnitude and sign that are strongly dependent on the degree of intramolecular rotation. Taking these into consideration, we believe that ThT represents an ideal molecular probe for the concerted ICD/DFT investigative approach. Since this method selectively reports on the fibril-bound ThT fraction, it could be a valuable alternative to the fluorescence amyloid assay, in particular for cases when the ThT–amyloid interaction leads to the formation of non-fluorescent complexes.^[64]

In this context, the scope of this review is to provide an account of the ICD investigations conducted over the years that deal with interactions of ThT in amyloid and other biologically relevant systems, while pointing out current pitfalls and ongoing challenges. Such a systematization of reported works is currently missing, and for this reason we consider this review to be a valuable contribution to spectroscopists performing amyloidosis-related research.

Even as spectroscopic techniques progress and new techniques become available, key aspects of the ThT–amyloid interaction continue to be debated in literature. These include the molecular form of bound ThT – monomer, dimer or higher aggregate, and the localization of the binding site(s) on the fibril. Several hypotheses have been put forward that are addressed in this review, as we explore the capabilities of the ICD method, assisted by DFT calculations, to shed light into these aspects. We also discuss critically the possibilities offered by the ICD/DFT approach to avoid some interference effects observed in fluorescence assays, such as self-quenching of ThT emission and bias caused by exogeneous species. Based on the available data, we assess the validity of using the ICD signature of ThT as an amyloid diagnostic tool complementary to fluorescence.

The review is structured as follows. The initial section is dedicated to the fundamentals of the molecular rotor behaviour of ThT, which plays the critical role in chirality induction. Then, after a brief recall of the basic principles of ICD, we examine a significant number of literature works that discuss chirality-inducing interactions of ThT with proteins, peptides, polyamino acids, polyanions and biocompatible gels. We focus on the efficiency of ThT as ICD molecular probe in bypassing the complexity of the systems to report on amyloid formation. Computational assessments of ICD signals are outlined next, ranking from simple host models like cyclodextrins or cucurbiturils to protein systems. The works corroborating ICD data with DFT results are discussed in detail. Lastly, conclusions are drawn and future perspectives are envisaged.

The molecular rotor behaviour

Here we discuss, in brief, the photophysics and spectral signature of ThT that originate in its behaviour as molecular rotor. Understanding the mechanisms that operate in ground and excited states for free ThT and for ThT in interaction with macromolecular partners is essential for the accurate interpretation of its induced circular dichroism signals, and for identifying the key complementary information to fluorescence that they can provide.

Structurally, the ThT molecule consists of a benzothiazole fragment connected to a dimethylaniline ring through a $\sigma(C-C)$ bond that allows intramolecular rotation around dihedral angle θ (**Figure 1**). Other important structural features are the positive charge at the azolic nitrogen atom (at pH < 10;^[76,77] please refer to the Supplementary Material 1 associated to ref.^[78] for the pKa determination of ThT), the reactive carbon atom in the thiazole ring, and the tertiary dimethyl amino group in the benzyl ring, the latter also associated to a torsional degree of freedom, ψ .

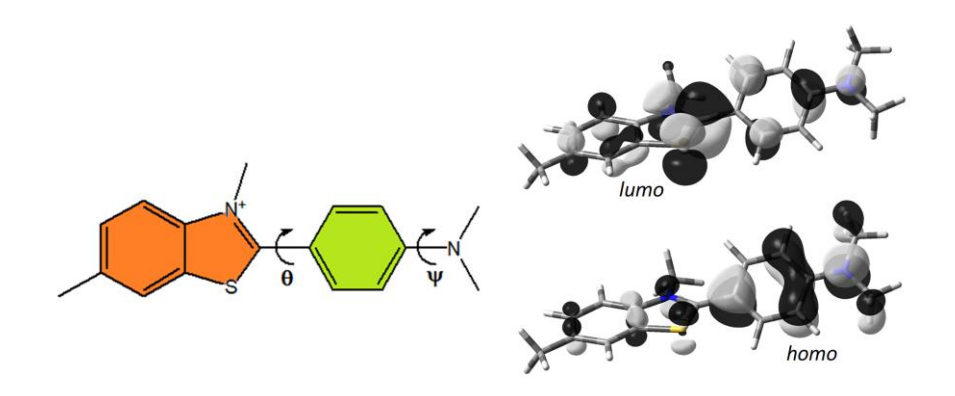


Figure 1. Left: Molecular structure of thioflavin T (ThT), with arrows illustrating intramolecular rotations about two dihedral angles, θ and ψ . Right: Frontier molecular orbital surfaces (isovalue 0.35 e/au³) for the most stable ground state conformer (θ = 37 deg, ψ = 0 deg) calculated at the B3LYP/6-311++G(d,p) level of theory.

In the early nineties, the research groups of Naiki^[79] and LeVine^[80] unearthed the fluorescent and binding properties of ThT, in the context of testing this molecule as an amyloid-specific fluorescent probe (histochemical dye), as had been proposed about forty years prior by Vassar and Culling.^[81] Upcoming years witnessed a surge of investigations debating the photophysics of ThT in solvents and solvent mixtures of different polarity/protic properties^[82–85] and viscosity,^[86–88] at variable pH and temperature,^[76,89] in ionic liquids^[90,91] and in deep eutectic solvents,^[92] as well as the spectral response of ThT during interaction with confining media such as host cavitands (cyclodextrins,^[93–96] cucurbiturils,^[97] calixarenes^[98]), micelles,^[99–101] metal-organic frameworks,^[102] bile salts,^[103] DNA/RNA,^[104–109] peptides,^[110–112] proteins in native^[113–115] or fibrillar^[116–118] state and, more recently, in gelling systems.^[119–121] The sensitivity of the ThT absorption and emission (in terms of band position, fluorescence quantum yield and lifetime) to the properties of the microenvironment, allowing ThT to probe the above variety of (supra)molecular systems, relies on its behaviour as molecular rotor. This was firstly revealed by Voropai *et al.*^[82] based on semiempirical PM3 quantum chemical calculations, and later documented in numerous experimental and theoretical studies.^[16,122–125]

Briefly, molecular rotors are fluorophores susceptible to forming twisted intramolecular charge transfer (TICT) excited states upon light absorption. [126] Two competing deexcitation pathways can follow: i) radiative decay, by emission of fluorescence from the first locally excited (Franck-Condon) singlet state (S₁/LE), and ii) non-radiative decay, by torsional relaxation, to a weakly emissive TICT excited state, and subsequent quenching of fluorescence. For ThT, the main nonradiative pathway has been shown to be the torsional relaxation about angle θ.^[127,128] Semiempirical AM1 and PM3 data^[82,122] and density functional theory (DFT) results at the 6-311+G(d,p) level of theory [127,128] suggest that the twisting of the dimethyl amino group with respect to the benzene ring is energetically prohibited in excited state by a four times higher rotational barrier as compared to the twisting of the dimethylaniline fragment [122,123] (Figure 2). A spectral signature identical to that of ThT was observed for a ThT derivative that was specifically designed having prohibited intramolecular rotation around the C-N bond, allowing the authors to conclude that torsional relaxation about angle ψ has very little influence on the emissive properties of ThT. [128] Nevertheless, more recent reports [129,130] coupling femtosecond transient absorption and femtosecond time-resolved fluorescence with TDDFT calculations draw attention to the existence of a dual relaxation channel for the S_1/LE state of ThT. The second relaxation pathway is non-radiative and involves an additional TICT excited state formed upon torsional relaxation along the dimethylamino coordinate, which is energetically favoured in the solvent methanol.

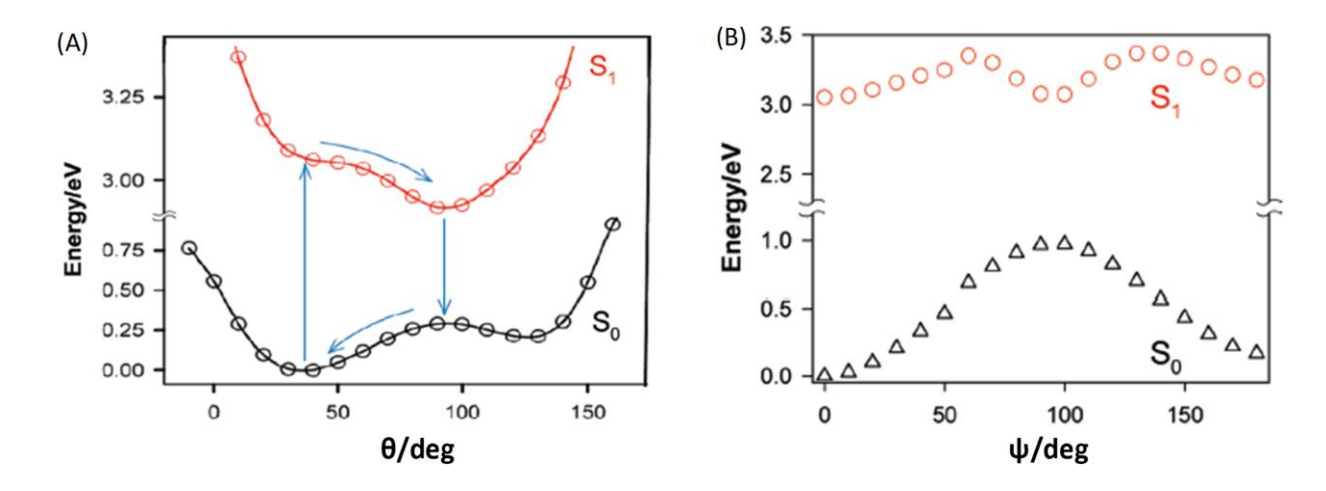


Figure 2. Sections through potential energy surfaces with respect to torsion angles θ (A) and ψ (B). Adapted with permission from ref.^[127] P. K. Singh, M. Kumbhakar, H. Pal, S. Nath, Ultrafast bond twisting dynamics in amyloid fibril sensor, J. Phys. Chem. B 114(7) (2010) 2541–2546. doi:10.1021/jp911544r. Copyright 2010 American Chemical Society; colour online.

In non-viscous solution, rotation about angle θ proceeds unhindered, and nonradiative deexcitation takes precedence over fluorescence emission. This results in a low fluorescence quantum yield ($\varphi \sim 0.0001^{[132]}$) and a short fluorescence lifetime ($\tau \sim 1$ ps^[87,131–133]) of ThT in water, at room temperature. By difference, in confining media – either in a viscous solution or upon an interaction that hinders intramolecular rotation, torsional relaxation is obstructed and a sterically favoured ThT conformation is "locked". Emission from the S₁/LE state of this conformer occurs, characterized by a 2–3 orders of magnitude higher fluorescence quantum yield ($\varphi = 0.28$ in rigid isotropic solution, $\varphi = 0.43$ in amyloid fibril^[131]) and lifetime ($\tau = 0.48$ ns in glycerol^[131]) as compared to ThT in aqueous solution. This type of straightforward on/off, concentration-dependent response upon binding to a macromolecular interaction partner^[134,135] constitutes the basis for using ThT as fluorescent staining reagent in amyloid assays. The fluorescence enhancement is also accompanied by large bathochromic shifts in the absorption and fluorescence maxima that serve as spectral fingerprints of the processes taking place.^[87]

At room temperature, ThT presents a wide distribution of conformations, from perpendicular ($\theta \sim 90$ deg) with broken π -electron conjugation that display absorption and emission bands at shorter wavelengths, to quasi-planar conformers responsible for the long wavelength absorption and emission. In homogeneous solution, conformer populations are determined by temperature and solvent polarity, while in heterogeneous systems, the conformer distribution is decided by the local properties of the microenvironment. The most stable conformers of ThT can be identified by plotting sections through potential energy surfaces built with respect to angle θ , in electronic ground state, θ , and first excited singlet state, θ , (Figure 2A). In θ , the minimum energy conformation corresponds to a value θ = 37 deg, a compromise between the planar (θ = 0 deg) conformer favoured by electronic effects and the steric hindrance introduced by the presence of a methyl substituent at the azolic nitrogen atom. Nevertheless, the value of 37 deg allows for an extended θ electron conjugation in the molecule. Quantum chemical calculations at semiempirical and ab initio levels evidenced the charge transfer occurring upon excitation from the highest occupied molecular orbital (homo), localized on dimethylaniline, to the lowest unoccupied molecular orbital (lumo), localized on benzothiazole (Figure 1).

In water, the absorption band associated with the *homo-lumo* Franck–Condon transition shows a maximum at 412 nm, and the corresponding π - π * transition electric dipole moment is polarized along the long axis of the molecule. The maximum energy conformation in S₀ state corresponds to θ = 90 deg. The energy barrier to rotation between the 37 deg and 90 deg conformers is low (~5 kcal/mol^[123,125]), the two molecular fragments rotating freely about the σ (C–C) bond. In S₁, the energy minimum corresponds to a conformer having θ = 90 deg (the TICT excited state)^[122] (**Figure 2A**). Upon excitation, the ThT molecule crosses to this TICT state, the nonradiative deexcitation pathway resulting in the weak fluorescence emission observed experimentally. This mechanism is favoured by the negligible energy barrier between the S₀/37 deg and S₁/90 deg conformers.^[16,127,133]

Perusing these studies, it becomes evident that the molecular rotor behaviour of ThT has been largely exploited in conjunction with the emissive properties of the dye. We must nonetheless take note of the fact that the presence of twisted conformations opens the way for an additional spectroscopic means of assessing the diverse binding interactions of ThT: induced circular dichroism – the primary focus of this review.

Induced circular dichroism as investigative method complementary to fluorescence

Compared to the exhaustive collection of fluorescence studies exploiting, thorough particular techniques, the emissive features of ThT derived from its molecular rotor behaviour, the number of reports addressing the dichroic signal induced to ThT upon interaction is considerably smaller. This is somewhat surprising, considering that circular dichroism is one of the go-to methods for characterising structural transitions in DNA^[28,138] and protein, ^[6,11,139,140] with emphasis on misfolding and aggregation. Such studies focus on revealing changes in the secondary and tertiary protein structures occurring upon fibril formation, and we consider that they could be well enriched with complementary insight provided by the induced circular dichroism (ICD) signal of the molecular probe counterpart – ThT in the case of amyloid assays.

An explanation for the limited number of ICD investigations may lay in the elements of difficulty inherent to performing dichroic measurements in anisotropic samples that possess light scattering properties and are prone to undergo precipitation. The well-known prerequisite for a correct analysis of extrinsic dichroic signals of proteins is the accurate determination of the protein concentration. This is not always straightforward, due to protein aggregation and subsequent sedimentation. Performing measurements under stirring or using dry samples are the workarounds commonly recommended. [20] In the case of ICD signals, which have inherent low intensity, [141] it is imperative, for a correct interpretation, to discern the signals originating from true chirality at molecular scale from those arising from a macroscopic, temporary alignment of chromophores. Such artefacts may ensue from optical effects like linear dichroism, when the incident light is not completely right or left circularly polarized, but contaminated by linearly polarized light,[142] and linear birefringence, caused by the inherent optical imperfections of the spectropolarimeter. [143] Fortunately, recent literature offers detailed guidelines on how to conduct experiments in order to eliminate these effects, [5,137,144-^{146]} therefore providing the ICD technique with the potential to become, in the near future, a widespread complementary tool for detecting the intercalation modes of probe molecules within proteins as well as other chiral environments. Since alterations in the local chirality of a macromolecule can often lead to dramatic changes in its biological activity, it becomes evident that such ICD studies are exceedingly necessary.

In what follows, the principle of ICD is briefly recalled, and the literature studies using ThT as ICD molecular probe are presented and discussed, emphasizing their implications for current amyloid assays. For a detailed view on circular dichroism spectroscopy, the reader is referred to the comprehensive works of Berova

and Woody,^[147,148] which include the basic concepts of electronic circular dichroism and its many applications to the biomedical field.

Basic principles of induced electronic circular dichroism

The absorption, to different extents, of left- and right-hand circularly polarized light by a chiral, non-racemic chromophore or by an achiral molecule to which chirality has been induced results in elliptically polarized light, and thus the observation of either an extrinsic or an induced dichroic signal. [147,149] Since electronic circular dichroism is, in essence, an absorption phenomenon, the dichroic signal is observed in the light-absorbing spectral region of the chromophore, and its intensity is commonly expressed as ellipticity. Differently from the absorption band, an ICD band can have either positive or negative sign, and is very sensitive (in terms of shape, position and intensity) to conformational changes, thus providing a spectral fingerprint of the microenvironment, which spectroscopists may use to reveal otherwise inaccessible local structural changes.

To optically inactive probes, such as ThT, chirality can be induced by one of the following mechanisms: $^{[148]}$

- i) the "chiral twist" mechanism, for probes possessing one or more torsional degrees of freedom: conformational adaptation to the binding site *via* torsional motion followed by hindering of the degree(s) of freedom, resulting in a bound conformer that is rigid and chiral;^[52,53]
- ii) non-covalent interactions with a chiral environment, *e.g.*, a cavitand, that alter the electron density of the probe; an example is the host–guest inclusion complexation with cyclodextrins, leading to ICD features of the guest that are governed by the Harata-Kodaka rules.^[150–152] Several reports document the (natural or synthetic) cyclodextrin–ThT complexation by fluorescence spectroscopy,^[96,153,154], however only two follow the ICD of the ThT guest.^[155,156]
- iii) intramolecular exciton coupling: coupling of transition electric dipole moments belonging to chromophores of the same probe molecule;^[157]
- iv) intermolecular exciton coupling: coupling of transition electric dipole moments of chromophores belonging a) to probe molecules that are found in close proximity (< 10 Å) and in chiral arrangement relative to each other, e.g., dimers, aggregates, or b) to the probe molecule and to its interaction partner, e.g., aromatic residues, peptide bonds; [157–159]

Exciton coupling leads to the observation of characteristic bisignate ICD signals (two bands of similar intensity and opposite sign) that are either positive (an -/+ Cotton effect, *i.e.* a positive long-wavelength band and a negative short-wavelength band) or negative (an +/- Cotton effect); the maximum of the absorption band corresponds to the cross-point in the ICD spectrum of the exciton. [157–159]

As was already mentioned, dichroic signals have inherent low intensity. This is because they arise from often minute differences between the absorptivities for left and right circularly polarized light. Therefore, an essential condition for successful ICD determinations is the existence of a strongly absorbing chromophore. With a molar extinction coefficient $\varepsilon = 36000 \ M^{-1} \ cm^{-1}$ (in water)^[160] for the absorption band at 412 nm, the ThT probe abides to this rule.

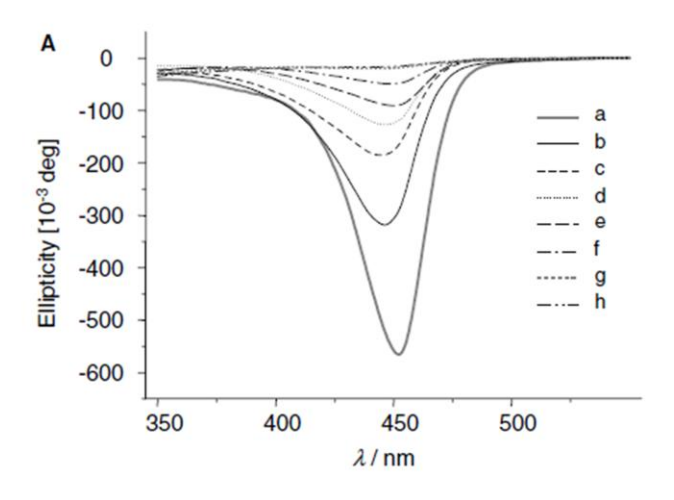
The intensity of the ICD signal is determined by the rotational strength of the corresponding transition^[147] that, in the particular case of ThT, is dependent on the value of the torsion angle θ . As expected, in water and other microenvironments that allow unhindered intramolecular rotation, the ThT monomer presents a zero net dichroic signal, as the mirror-image ICD signals of all non-planar conformers cancel each other out. The planar, "achiral" conformer ($\theta = 0$ deg) and the conformer twisted at right angle ($\theta = 90$ deg) do

not show ICD signals due to broken π -electron conjugation. ^[161] By difference, in restrictive microenvironments, one or more twisted, "chiral" conformers can be stabilized, leading to the observation of characteristic mono or bisignate ICD bands. It emerges evident one of the key advantages of ICD spectroscopy over traditional absorption: while the absorption spectrum is dominated by the unbound species, especially in cases when the association constant is low, the ICD spectrum exclusively reports on the bound ThT species acquiring chirality. There is also an evident advantage of ICD over the fluorescence method for which results can be biased by exogenous compounds present in the amyloid assay that alter the fluorescence response of ThT. Such interferences may arise from direct interaction leading to quenching of the ThT fluorescence, *e.g.*, by a Förster resonance energy transfer mechanism, from spectral effects like band superposition and inner filter, or from cooperative or competitive binding. ^[71,73]

Induced circular dichroism of thioflavin T bound to proteins, self-assembling peptides and polyamino acids

The excellent works by the research groups of Dzwolak and Pecul brought forth crucial advances in understanding the origin of ThT dichroic signals. Their studies are the first building blocks paving a promising way for ICD to become a new diagnostic tool for protein fibrillation. In 2005, they reported the first ICD signal of amyloid-bound ThT, observed in the presence of insulin fibrils.^[62] The signal consists of one negative band located at 450 nm, with intensity linearly dependent on the ThT concentration (**Figure 3A**). Prior to this study, no data was available in the literature regarding the use of ICD as spectroscopic tool for the characterization of the interaction of ThT with either native or pathological proteins. By determining that the variation in the ThT/amyloid molar ratio caused no alteration in the shape of the ICD signal, the authors were able to discard the formation of a chiral assembly of ThT molecules, easily destroyed by dilution. Instead, they concluded that the ICD signal originated from a twisted, optically active conformation of the bound ThT molecule. A follow-up study published in 2007^[5] consolidated the ICD method as an effective tool for investigating conformational effects in protein misfolding, adding knowledge on the topological organization and symmetry of the insulin amyloid fibril. These investigations also pointed out a noteworthy advantage of the ICD technique, namely that it allows experiments to be performed at high ThT concentrations of 1 mM. Such concentrations are unusable in fluorescence determinations due to self-quenching of the ThT emission.

Another pioneering study^[162] employed the ICD signal of ThT to evidence the vortex-assisted fibrillation of insulin occurring at 60°C. This was the first instance that a chiral symmetry-breaking process was observed in a biopolymer. The process, penned by its discoverers "chiral bifurcation", refers to the formation of two types of insulin fibrils with opposite chiral senses (denoted by –ICD and +ICD) that, upon binding of ThT, induce in the achiral probe opposite signs of the extrinsic Cotton effect. "Chiral bifurcation" of protein conformational transitions was shown to involve an autocatalytic mechanism in which a random conformational fluctuation triggers the conversion of a macroscopic amount of insulin into uniformly biased chiral aggregates that bind and twist the ThT molecule.



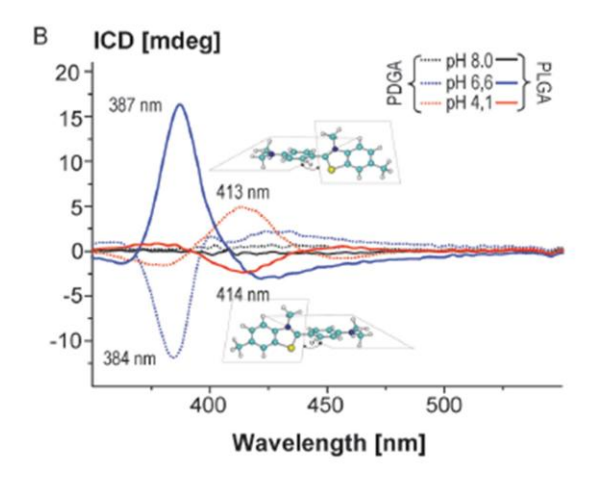


Figure 3. (A) The ICD spectra of ThT in the presence of insulin fibrils at different ThT/amyloid molar ratios: 1/1 (a), 1/2 (b), 1/5 (c), 1/10 (d), 1/20 (e), 1/50 (f), 1/100 (g), 1/200 (h). Used with permission of Elsevier, from ref. Chiral bias of amyloid fibrils revealed by the twisted conformation of Thioflavin T: An induced circular dichroism/DFT study, W. Dzwolak, M. Pecul, FEBS Letters, 579, 29, 6601–6603, 2005; permission conveyed through Copyright Clearance Center, Inc. (B) The ICD spectra of ThT in the presence of polyamino acids PLGA and PDGA in random coil (pH 8.0), intermediate (pH 6.6) and α-helical (pH 4.1) conformations. Used with permission of Royal Society of Chemistry, from ref. Thioflavin T forms a non-fluorescent complex with a-helical poly-L-glutamic acid, V. Babenko, W. Dzwolak, 47, 10686–10688, 2011; permission conveyed through Copyright Clearance Center, Inc.; colour online.

To aid in rationalizing the ICD features of ThT bound to insulin fibrils, the authors included in their reports data on the ICD observed for ThT in the presence of amyloid-like polyamino acids having opposite chirality. Mirror-image ICD signals were revealed for ThT bound to poly-L-glutamic acid (PLGA, -ICD) and to poly-D-glutamic acid (PDGA, +ICD) in their β -pleated, amyloid-like conformation, as well as for ThT bound to β -sheet-rich fibrils of poly-L-lysine (-ICD) and poly-D-lysine (+ICD). On the basis of these results, the authors proposed ThT as an apt molecular probe to report on chiral bias phenomena occurring in amyloid and amyloid-like structures.

In subsequent, more exhaustive studies, ThT was employed as ICD probe to characterize the PLGA structural transition from random coil to α -helix that occurs as a function of pH. [64] For this system, the information provided by fluorescence spectroscopy was scarce due to the fact that the ThT/PLGA complex is non-fluorescent. Data provided by absorption spectroscopy was equally limited, revealing only a small absorbance decrease upon structural conversion. The investigation by ICD was enlightening, as the features of the ICD signal of the ThT/PLGA complex proved to be distinct for the different conformations of the polyamino acid. For random coil PLGA (at pH 6.5), a strong positive ICD signal of ThT is observed at 387 nm, while for α -helical PLGA (at pH 5), a weaker negative ICD band, located at 414 nm, is revealed in the spectrum (**Figure 3B**). In what concerns the interaction mechanism, it was rationalized that, at pH 6.5, the negative charge on PLGA is the driving force of its electrostatic self-assembly with cationic ThT. The hypsochromic shift of the ICD signal in PLGA (387 or 414 nm) with respect to the ICD signal in insulin fibrils and in PLGA β_2 fibrils (450 nm) correlates with the different emissive properties previously observed for ThT in these systems. $^{[64,163]}$ It is indicative of the presence of several bound ThT conformers having different degrees of conjugation between the two molecular fragments, *i.e.* either intact or disrupted π -electron systems. The conformers with broken π -electron conjugation have spectral signatures close to those of the individual chromophores. $^{[123]}$ The ICD spectra of ThT

in PDGA are, as expected, mirror images of those obtained in the presence of PLGA in the same experimental conditions.

These results have two major implications. Firstly, by revealing that ThT binds orderly to α -helical structures, the authors demonstrate that ThT binding to protein targets is less amyloid-specific than initially assumed. While interactions with β -sheet structural motifs^[164] and/or π - π interactions with aromatic amino acid residues^[64] are still considered responsible for ThT binding to amyloid structures^[17] as they occur with higher affinities, care must be taken during amyloid assays to eliminate any possible bias arising from non-specific binding to native background proteins. Secondly, it is shown that ThT binding to amyloid structures, as revealed by the immobilization of ThT in a chiral conformation, is not a prerequisite for fluorescence enhancement. That is, a bound ThT conformer that is weakly fluorescent or non-fluorescent may give rise to a strong ICD signal, demonstrating complexation. This observation is key for the complementarity of the two spectroscopic techniques. When used in tandem with fluorescence, the ICD method can provide a means to check whether the binding of the molecular probe to the macromolecular partner results in the formation of a non-fluorescent complex that may bias the quantitative results of the traditional fluorescent amyloid assay.

More recently, the authors recorded, for the first time, the circularly polarized luminescence spectrum of ThT bound to insulin fibrils.^[137] Their study demonstrated that the induced chirality existing in ground state is retained in the emissive excited state of ThT. The sign of the Cotton effect in the circularly polarized luminescence spectrum is the same as that in the ICD spectrum. Future studies can be envisioned, as the intense circularly polarized luminescence of ThT may find diverse applications in asymmetric synthesis, sensors, and in display and optical storage devices.^[166]

The research group of Sabaté has undertaken an investigation^[78] aimed at determining whether the Cotton effect observed by Dzwolak and Pecul with insulin^[62] is a general property of fibril-bound ThT. As opposed to insulin, which is a short peptide of 51 amino acids, Sabaté *et al.* selected for their study the larger HET-s protein, namely its 72 amino acid prion forming domain, HET-s(218–289), which assembles into fibrils at pH 2.^[167] HET-s(218-289) is one of the few amyloid proteins for which the structure of the fibrillar state is available at high-resolution.^[168,169] The appearance of a negative ICD band at ~450 nm was observed, similar in terms of sign and position to that recorded for insulin, but differing in terms of asymmetry (**Figure 4**). The latter feature may be an indication of a slightly different population of conformers being stabilized in HET-bound ThT as compared to insulin-bound ThT, and constitutes proof that ThT can report on the heterogeneity of the binding site. Corroborating the experimental ICD data with computational results^[62] that will be discussed in detail later in the review, the left-handed twist of HET-s fibrils was inferred.

The authors conclude that the chirality imposed to the ThT probe upon binding is a general feature of the ThT–amyloid interaction. They point out that the features of the ICD signal can aid in clarifying the binding mode of ThT to amyloid fibrils, a subject of continuous debate in the literature over the years. Based upon current knowledge, it is reasonable to state that ThT does not bind to the amyloid fibrils in micellar form, as previously suggested by Khurana *et al.* on grounds of fluorescence results. [170] Binding as a dimer was proposed by Groenning *et al.* [160,171,172] but seems equally unrealistic in the case of insulin [173] and HET-s, since no bisignate signal, attributable to the ThT–ThT exciton coupling mechanism, is observed. Instead, the ICD results support the hypothesis of ThT binding along the fibril's long axis, either in hydrophobic channels or at the protofilament interface, a mechanism that was proposed by Krebs *et al.* [15] on the basis of confocal microscopy data. Such a binding mode can impose preferential twisted conformations of the bound ThT monomers. Measurements of fluorescence polarization, quantified using emission dichroism, allow distinction between the monomer, dimer (excimer) and micelle emissions of ThT on the basis of their unique spectral signatures. For the system

ThT/insulin, these measurements support the Krebs binding model, indicating that ThT binds in monomeric form to the β -sheet grooves that run parallel to the fibril's long axis. [174]

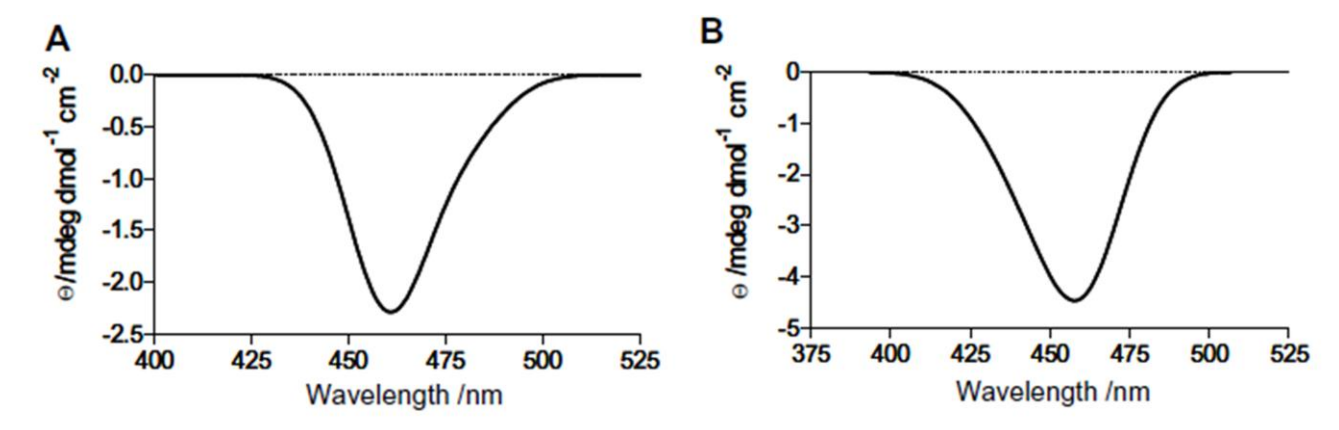


Figure 4. The ICD spectra of ThT bound to (A) insulin fibrils and (B) HET-s(218–289) fibrils. The concentrations of ThT and fibrillar protein are 0.5 mM. Reprinted from ref.^[78] J. Struct. Biol., 162/3, R. Sabaté, I. Lascu, S. J. Saupe, On the binding of Thioflavin-T to HET-s amyloid fibrils assembled at pH 2, 387–396, Copyright (2008), with permission from Elsevier.

Biancalana *et al.* evidenced the same negative ICD signal of ThT in the presence of some peptide self-assembly mimic scaffolds. [175] Such scaffolds are constructed with the intention of obtaining simpler model systems for the β -sheet rich ThT binding site on amyloid fibrils. [176] They possess the advantages of lower heterogeneity and increased solubility, which makes them amenable to various spectroscopic and biochemical methods of investigation. The ICD band arising from the twisted ThT conformers bound to these peptides is observed in the 420–440 nm spectral region, depending on the scaffold type.

Notable advances have been brought forth by Zsila with his expertise of over 25 years in decoding ICD signals arising from a multitude of biologically relevant interactions. Discussed here is one of the first reports on the ICD of ThT, observed upon binding to chicken α_1 -acid glycoprotein (cAGP),^[113] as well as the most recent study focused on the interaction of ThT with sulfated glycosaminoglycans (GAGs).^[63]

The cAGP transport protein shares the common structural motif of the lipocalin family, a central β -barrel cavity serving as main binding site. Inclusion of ThT within this cavity generates a negative ICD band at ~430 nm (Figure 5A). [113] A large bathochromic shift (~20 nm) is observed in both the ICD and absorption spectra of bound ThT as compared to free ThT, associated with a 585 cm⁻¹ decrease in the full width at half maximum of the absorption band. These spectral changes can be rationalized in terms of the stabilisation of a subset of bound ThT conformers adopting a more planar geometry that enhances the π -electron conjugation between the benzothiazole and dimethylaniline fragments, subsequently decreasing the *homo-lumo* gap. Computational data support this assertion as they predict a low energy barrier to rotation of 13.2 kJ/mol between the equilibrium conformer (θ = 34.6 deg) and the planar conformer. [62]

Importantly, Zsila's studies have shown that the utility of ICD experiments using ThT or other spectral probes does not limit to qualitative assertions, but extends to collecting quantitative data on the binding process, such as the value of the association constant and the number of binding sites. This can be done by fitting the ICD data with binding models described in the literature for different stoichiometries of the interaction, and selecting the most appropriate model in terms of statistical parameters. [177,178] In the case of the ThT/cAGP system, the values for the association constant and for the number of binding sites, obtained in pH 7.4 phosphate buffer, at 25°C, are 4.34(±0.14)×10⁶ M⁻¹ and 0.74, respectively. [113] Competitive or displacement experiments can also be performed in order to identify the localization of the binding site of ThT. [140,179] Such measurements rely on the disappearance of the ICD signal of the spectral probe of interest

upon addition of a competing ligand that binds to the same protein pocket with higher affinity. ^[147,180] To obtain accurate results, it is important not to have interfering signals (either extrinsic or ICD) from the competing ligand.

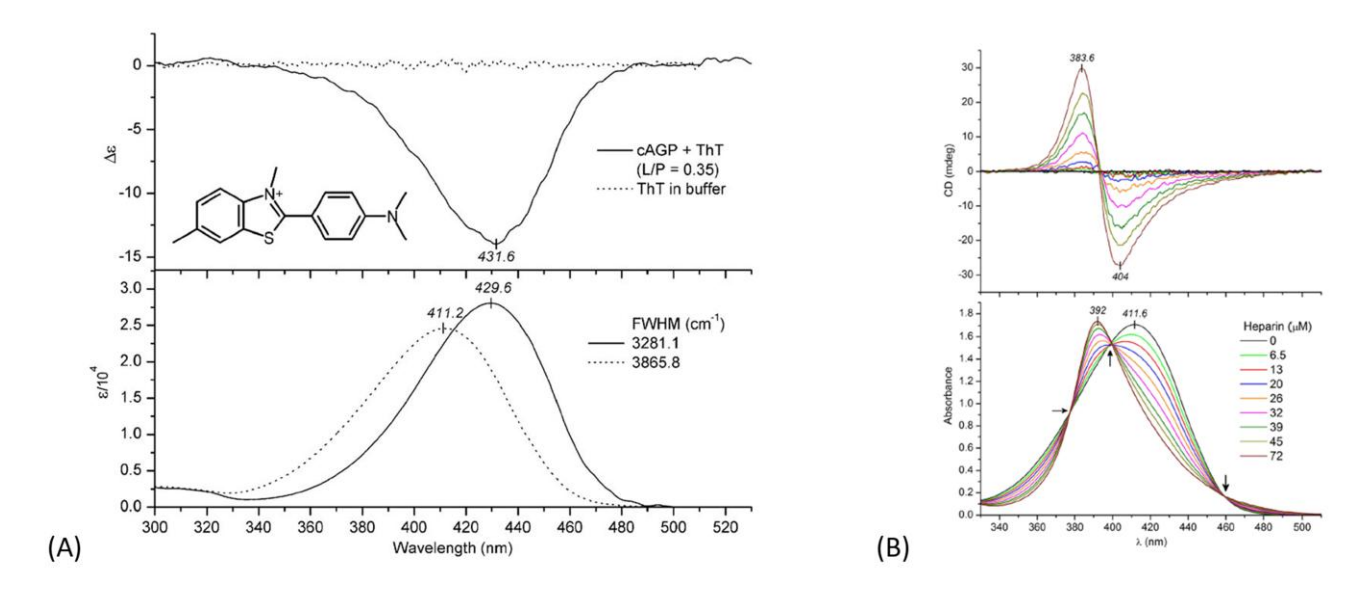


Figure 5. (A) The ICD (upper) and absorption (lower) spectra of ThT in the absence and in the presence of cAGP at pH 7.4; [cAGP] = 47 μM. FWHM denotes the full band width at half of the absorption maximum. Reprinted from ref.^[113] Biochim. Biophys. Acta, 1760/8, F. Zsila, H. Matsunaga, Z. Bikádi, J. Haginaka, Multiple ligand-binding properties of the lipocalin member chicken α1-acid glycoprotein studied by circular dichroism and electronic absorption spectroscopy: The essential role of the conserved tryptophan residue, 1248–1273, Copyright (2006), with permission from Elsevier. (B) The ICD (upper) and absorption (lower) spectra of ThT in the absence and in the presence of increasing concentrations of heparin in deionised water; [ThT] = 55 μM. Reprinted with permission from ref.^[63] F. Zsila, S. A. Samsonov, M. Maszota-Zieleniak, Mind your dye: The amyloid sensor Thioflavin T interacts with sulfated glycosaminoglycans used to induce cross-β-sheet motifs, J. Phys. Chem. B 124(51) (2020) 11625–11633. doi:10.1021/acs.jpcb.0c08273. Copyright 2020 American Chemical Society; colour online.

Induced circular dichroism of thioflavin T bound to glycosaminoglycans and other polyanions

The recent investigation by Zsila *et al.*^[63] on the interaction of ThT with two GAGs, heparin and chondroitin 6-sulfate, was spurred by the fact that GAGs intervene in a multitude of normal and pathological mechanisms, and are often used to promote fibril formation in studies of amyloidogenesis. If ThT is added to GAG-containing systems, clearly the mechanism of its interaction with the GAGs themselves should be known. The authors have shown that the presence of either heparin or chondroitin 6-sulfate determines the appearance of a strong +/- bisignate ICD signal of ThT, pointing to an exciton coupling interaction mechanism. The negative Cotton effect is observed at +(384 nm)/-(404 nm) for heparin (**Figure 5B**) and is indicative of a left-handed (counterclockwise) arrangement of ThT conformers, with individual transition moments oriented parallel to each other, stabilized by π - π stacking interactions. The hypsochromic shift observed in the absorption spectrum is characteristic for the formation of H-aggregates that have head-to-head arrangement. Association of cationic ThT to heparin is driven by electrostatic attraction to the anionic sites (sulfate, carboxylate) of the GAG, which are helically arranged along its linear chain. It is also possible for

the asymmetric centres of the sugar residues to play a role in the observed ICD. In the case of chondroitin 6-sulfate, a more loosely packed arrangement of bound ThT conformers is proposed based on the different features of the absorption spectrum as compared to heparin (smaller hypsochromic shift, fewer isosbestic points), and is corroborated by molecular dynamics results. This hypothesis is accounted for by the lower negative charge density of chondroitin 6-sulfate. From the intensity of the ICD signals, the apparent dissociation constants for the ThT/heparin and ThT/chondroitin 6-sulfate systems were evaluated at ~35 μ M. Since the main conclusion of the study is that the ThT/amyloid binding equilibrium can be altered by concurrent ThT/GAG interactions, the authors warn on the importance of selecting appropriate experimental conditions when performing tri-component assays containing cationic amyloid-sensing probes, amyloid fibrils and GAGs. The suggested workaround is to perform the assay in the presence of sodium ions at previously determined concentrations instead of in pure water as is the current norm. By destabilizing the ThT/GAG complexes *via* Coulombic shielding of the anionic sites on the GAG chain, the presence of sodium ions should eliminate any bias induced by ThT binding to the GAG.

It is important to mention that, prior to Zsila *et al.*, Mudliar and Singh conducted a study on the interaction of ThT with heparin and chondroitin sulfate,^[181] in which they obtained no evidence of an interaction occurring between ThT and chondroitin sulfate on the basis of steady-state and time-resolved fluorescence measurements alone. Once more, this points to the necessity of adding ICD as diagnostic tool complementary to fluorescence.

The same authors later developed an ingenious ICD ratiometric sensor for the detection of two amino acids with basic character, arginine and lysine, based on them competing with ThT for the same heparin binding site.^[184] The higher affinity of these amino acids for heparin determines the dissociation of the ThT/heparin complex, a process that can be followed in the ICD spectrum. Upon increasing the amino acid concentration, the gradual decrease in the intensity of the negative +/– bisignate signal of heparin-bound ThT is observed, culminating with its complete disappearance. A similar displacement of ThT from its complex with heparin was observed in the presence of protamine, a low molecular weight protein used to treat heparin overdoses.^[180]

Differently from the case of GAGs, the interaction of ThT with another chiral polyanion, polyadenylate, leads to the observation of a positive Cotton effect at –(402 nm)/+(422 nm).^[185] This study by Fedunova *et al.* brings forth an observation of value for researchers attempting ICD studies on ThT, namely that the interaction of ThT with achiral polyanions like polystyrene sulphonate, polyacrylate or polyvinyl sulfate, although confirmed by UV-Vis absorption and fluorescence measurements, ^[183,186] does not lead to the observation of an ICD signal. ^[185] This emphasises that, in complexes with flexible polyanions with random structure, the dominant role in generating chirality is played by the chiral template provided by the host environment, and not by the conformation of the ligand itself. This interplay between the "chiral twist" and the electronic mechanisms in generating chirality has been discussed by our group for the case of host–guest inclusion complexes with cyclodextrins. ^[187]

Polyadenylate is one of the simplest polynucleotides. The mechanism of interaction of ThT with nucleic acids has been documented by fluorescence^[188,189] as well as other techniques including circular dichroism on the extrinsic band of DNA.^[26] Alongside typical dichroic signals of DNA in the 200–350 nm spectral region, there is one report mentioning ICD signals of ThT recorded in the presence of DNA.^[106] In this work, ThT was shown to induce folding of human telomeric DNA into either parallel or antiparallel G-quadruplex structures. Concomitantly with the topological change from antiparallel to parallel, the positive ICD band of ThT at ~450 nm transforms into a negative ICD band shifted hypsochromically to ~440 nm (**Figure 6**). The process is influenced by the concentration of Tris buffer, and is favoured by the presence of metal ions like Na⁺ and K⁺.

These changes in the features of the ICD spectrum reveal different microenvironments and different interaction modes experienced by ThT upon binding to DNA, due to distinct topologies of the antiparallel and parallel quadruplex structures. Recently, Xue *et al.*,^[190] while using circular dichroism to improve the feasibility of their electrochemical/fluorescent dual-sensing platform, recorded a similar, positive ICD band of ThT at ~450 nm in the presence of antiparallel G4 target DNA. On a side note, electrochemical techniques^[191–194] have been proven effective in monitoring amyloid formation by following the oxidation of ThT and other benzothiazole dyes,^[195] and in screening for new dye/inhibitor pairs to be used in amyloid assays.^[196]

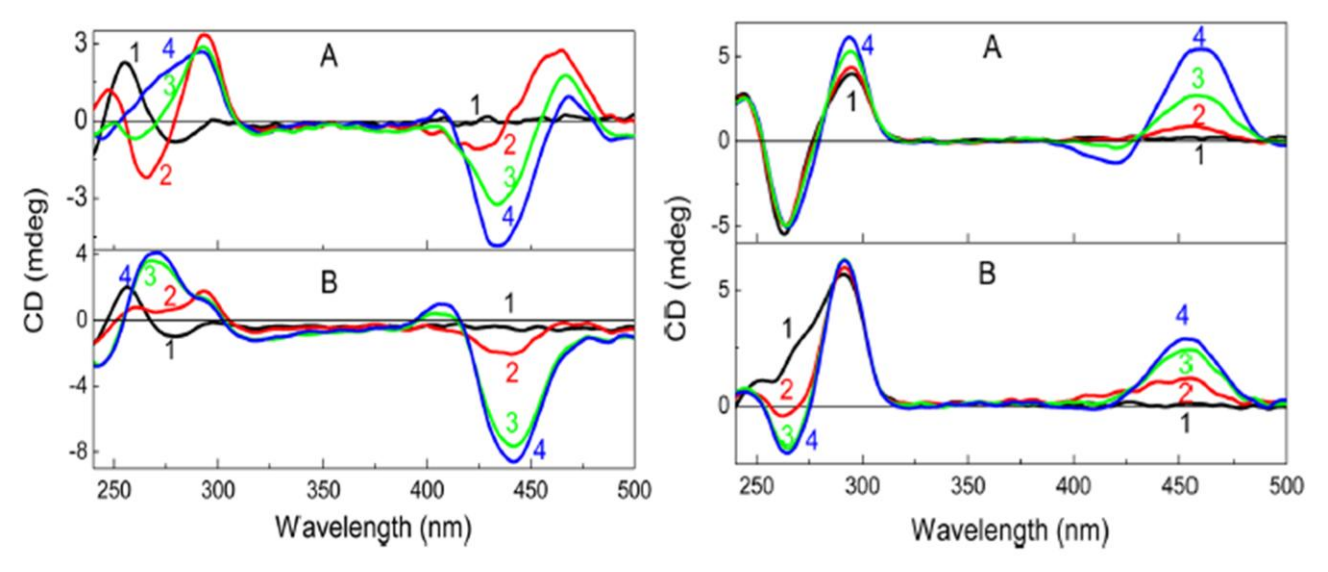


Figure 6. Circular dichroism spectra of 22AG DNA (12.5 μM). Left: Tris buffer (pH 7.2) is (A) 5 mM and (B) 50 mM; ThT is (1) 0 equiv; (2) 2 equiv; (3) 4 equiv; (4) 8 equiv. Right: Tris buffer (pH 7.2) is 50 mM; salt is (A) NaCl (50 mM); (B) KCl (50 mM); ThT is (1) 0 equiv; (2) 2 equiv; (3) 4 equiv; (4) 8 equiv. Reprinted with permission from ref.^[106] J. Mohanty, N. Barooah, V. Dhamodharan, S. Harikrishna, P. I. Pradeepkumar, A. C. Bhasikuttan, Thioflavin T as an efficient inducer and selective fluorescent sensor for the human telomeric G-quadruplex DNA, J. Am. Chem. Soc. 135(1) (2013) 367–376. doi:10.1021/ja309588h. Copyright 2013 American Chemical Society; colour online.

Induced circular dichroism of thioflavin T in biocompatible gelling systems

To date, the only application regarding the generation of an ICD signal of ThT in a gelling system comes from the group of Mata. [197] In an interesting study from 2019, the authors report on the self-assembly of nanofibers formed by a peptide amphiphile (PA-E3) with a low-molecular-weight gelator, the carboxylate derivative of 1,3(R):2,4(S)-dibenzylidene-D-sorbitol (DBS-COO⁻). The hydrolysis of glucono- δ -lactone to gluconic acid provides the slow acidification conditions necessary to trigger the gelation of DBS-COO⁻, and the slow protonation of the carboxylate groups of both DBS-COO⁻ and PA-E3 directs the gradual self-assembly; PA-E3 self-associates due to a combination of hydrophobic interactions (between the palmitoyl chains attached to the peptide backbone) and electrostatic interactions (between the charged head groups), while DBS-COO⁻ forms intermolecular hydrogen bonds between the sugar units and participates in π - π stacking interactions. Based on this kinetically controlled process, the authors design supramolecular hydrogels with tunable mechanical properties. The ICD response of ThT is the key in following the gelation process, which occurs over a time course of 4 hours (**Figure 7**). Incorporation of ThT into the emerging gel network gives rise to a dichroic signal as the rigidity imposed by the gel fibres increasingly hinders intramolecular rotation. It is somewhat surprising

to note that the intensity of the ICD signal is quite large compared to that of ThT in the other chirality-inducing systems discussed. The time evolution of the ICD spectrum reveals a combination of two distinct chiral signatures, one of ThT in PA-E3 (a decreasing negative band at 385 nm and an increasing negative band at 470 nm) and the other of ThT in DBS-COOH (a negative +(370 nm)/–(385 nm) Cotton effect), as well as the increase of a new positive band at 450 nm. This is a striking observation, which points to the conclusion that ThT can sense the different chiral environments present in the gel structure. Importantly, this study suggests that the ICD property of ThT could be used in kinetic studies to follow the time course of amyloid growth, on a similar premise as that applied to fluorescence measurements, that the quantity of bound ThT is proportional to the quantity of fibrils formed. It is also expected for this study to be followed by other investigations exploring the capabilities of the ICD response of ThT in diverse gelling systems. The second derivative of the steady-state and synchronous fluorescence of ThT have already been successfully exploited by us in order to accurately measure the critical gelation temperature of some emerging pluronic F127/polysaccharide gelling materials. [198]

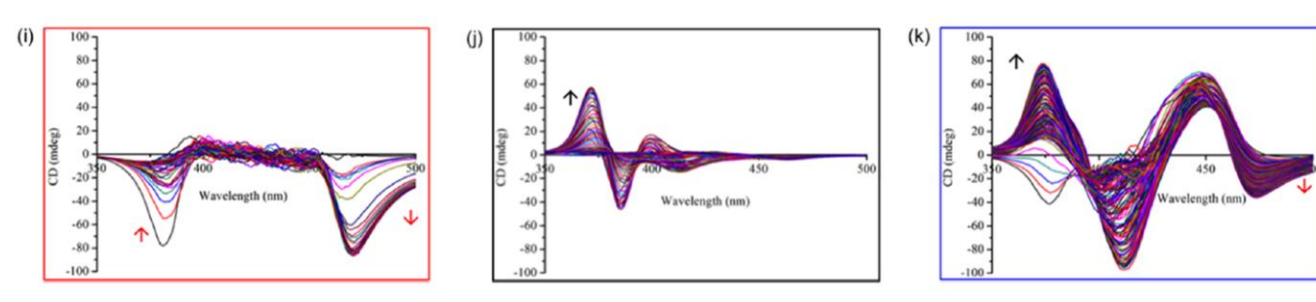


Figure 7. The ICD spectra of ThT, acquired at a 2 min interval, during the self-assembly of (i) PA-E3, (j) DBS-COOH, and (k) PA-E3/DBS-COOH. The arrows indicate the time evolution of the spectra. Reprinted with permission from ref.^[197] B. O. Okesola, Y. Wu, B. Derkus, S. Gani, D. Wu, D. Knani, D. K. Smith, D. J. Adams, A. Mata, Supramolecular self-assembly to control structural and biological properties of multicomponent hydrogels, Chem. Mater. 31(19) (2019) 7883–7897. doi:10.1021/acs.chemmater.9b01882. Copyright 2013 American Chemical Society; https://pubs.acs.org/doi/10.1021/acs.chemmater.9b01882; colour online.

Circular dichroism induced to other amyloid-specific dyes during protein structural changes

Promising results that further demonstrate the capability of the ICD method to reveal conformational changes in proteins have been reported with two other amyloid dyes possessing rotational degrees of freedom, Congo red^[180] and, recently, 8-anilinonaphthalene-1-sulfonic acid (ANS).^[199]

The ICD response of Congo red upon interaction with bovine serum albumin (BSA) was investigated during thermal treatment of the protein in the temperature range 30–90°C, in the presence of site I (warfarin, phenylbutazone) or site II (ibuprofen, naproxen, dansylglycine) markers. [180] The increase in temperature determined a decrease in the intensity of the ICD band of Congo red at 490 nm, concomitantly with the increase of a new band at 536 nm. Such spectral features indicate that the dye is subjected to a conformational change rather than to dissociation from the binding pocket of the protein, as the latter would result in a complete loss of ICD signal. By fitting the ellipticity values at either wavelength to a sigmoid function, the midpoint temperature of the native-to-amyloid structural transition was determined at 58°C. This value corelates to that obtained following the extrinsic circular dichroism signal of BSA in the spectral domain that reveals changes in the tertiary structure of the protein. This study marks the first successful investigation of a native-to-amyloid structural transition undertaken using the temperature-dependent alterations of the ICD

spectrum of a protein-bound molecular probe. The authors highlight the utility of such an experimental protocol that allows real time monitoring of protein aggregation.

In the study employing ANS,^[199] DFT calculations and principal component analysis complement the ICD study performed at variable temperatures in the range 20–80°C, revealing gradual conformational changes that occur during two different thermal denaturation pathways of BSA (as a model for self-crowding media) and lysozyme (model for surface binding).

Interesting results reported recently by de Carvalho Bertozo *et al.*^[200] can spur new applications of the ICD method to amyloid studies. By observing an inversion in the ICD signals of two dimers of vanillin and methyl vanillate, the authors demonstrated the displacement of these molecular probes from their binding site on BSA to the binding site on human serum albumin. On this basis, they propose to use the ICD inversion property of these molecules to study albumin structural alterations caused by temperature. Extrapolating, we can assume other phenomena affecting the structural integrity of proteins could be investigated in this manner.

Along with ThT, which yields characteristic bisignate signals due to exciton coupling when two monomers are in close proximity, molecular probes that display ICD inversion can be of use in monitoring in real time the structural evolution of intermediates formed during amyloid disaggregation. This is a mechanism under consideration as treatment option for amyloidosis. Disaggregating agents like heat shock proteins or small molecules (polyphenols, osmolytes) can be used to break down amyloid aggregates into oligomers and monomers. Nevertheless, the mode of action and resulting products of these agents must be characterized at molecular level, as they could in fact exacerbate the disease due to an elevated cellular toxicity of amyloid oligomers. While the fluorescence assay may detect a decrease in ThT fluorescence upon disaggregation, the ICD method could provide more detailed information on the generation conditions and structure of disaggregation intermediates and products. This is due to the fact that, during this process, the molecular probe experiences different strand-to-strand or sheet-to-sheet interactions, which are expected to produce gradual changes in the ICD signal.

These findings accentuate the potential of the ICD technique for investigating amyloid-like fibril aggregates by employing not only ThT, but other amyloid dyes as well, and undoubtedly invite further studies.

As elaborated in our perspective article,^[52] the ICD technique becomes even more attractive for harvesting structural information when it is used in tandem with high level quantum chemical computational methods like (time-dependent) density functional theory, (TD)DFT. In the final section of this review, an account of the molecular modeling methods used to characterize the interactions of ThT with various macromolecular partners is presented, with emphasis on the reports corroborating DFT results with ICD data.

Computational assessment of chirality-inducing interactions of ThT

Computational methods of variable degrees of complexity have been essential tools in clarifying the molecular rotor behaviour of ThT, and in rationalizing the changes in its photophysics upon interaction with diverse macromolecular partners. In the particular case of amyloid assays, the interaction parameters determined experimentally could be interpreted on the basis of *in silico* simulations, to provide an atomic-scale rationale.

Some of the most relevant computational studies dealing with the molecular rotor behaviour of ThT have been addressed at the beginning of this review. The early theoretical investigations also concerned the inclusion complexation of ThT, as guest molecule, with cucurbiturils^[204] and cyclodextrins,^[154] as host cavitands. This type of non-covalent interaction has initially been explored by the semi-empirical PM3 method, which revealed the guest–host stoichiometries: 1:1 and 1:2 with CB7, 2:1 and 2:2 with the larger CB8 where ThT can

be included as excimer. [205] Recently, a more computationally expensive approach, ONIOM, has been applied by Kung et~al. [134] to rationalize the turn-on fluorescence response of ThT upon immobilization within the cavity of a β -cyclodextrin derivatized with seven carboxylate tails. The ThT high layer was described at the B3LYP/6-31+G(d,p) level of theory, while the PM6 semi-empirical method was used for the cyclodextrin low layer. Molecular docking was also used to support spectroscopic results regarding the effect of the cavity size of sulphated cyclodextrins on the ThT binding affinity; [96] a 1:1 stoichiometry was predicted for complexes with α -and β -cyclodextrins, while a ThT trimer was included in the larger γ -cyclodextrin cavity. A combined molecular docking/molecular dynamics procedure was reported for modeling a ternary ThT/ γ -cyclodextrin/sodium dodecyl sulfate complex. [206]

Several computational works were dedicated to the interaction of ThT with DNA, either by docking ThT to G4 DNA and RNA grooves^[108] or by applying molecular dynamics considering different binding poses of the ThT monomer to G-quadruplex DNA: antiparallel groove-binding (unstable complex), antiparallel or parallel end-stacking (energetically favoured complexes), antiparallel or parallel structure in dual binding mode (end-stacking and groove-binding), parallel groove-binding.^[106] The latter investigation revealed that antiparallel DNA can accommodate two ThT monomers, one in end-stacking mode and the other in groove-binding mode. The authors hinted at the fact that these dimeric structures might be responsible for the ICD bands observed experimentally (**Figure 6**). Complex quantum mechanics, molecular mechanics and molecular dynamics combined approaches have been undertaken by Biancardi *et al.*^[188,207] to evidence how the shape of the DNA binding site can influence intramolecular rotation in ThT upon binding. A complex interaction was revealed, involving an interplay of several binding modes: monomer intercalation, external binding/minor groove binding of ThT dimers. TDDFT calculations at the CAM-B3LYP/6-311+G(d,p) level for ThT and at CAM-B3LYP/6-31G level for the frozen geometries of the DNA pockets were applied to simulate absorption and fluorescence spectra.

One of the key advantages brought by computational simulations to the study of amyloids is the means to simplify these structurally complex systems by using minimalist molecular models that capture the properties of the fibrils by taking into account their repetitive nature. Such models can be used to identify preferential interaction sites and elucidate interaction mechanisms. An accessible model system describing the protofibrils formed by the Alzheimer peptide A β 16-22 was constructed by Wu *et al.*^[208] and investigated using molecular dynamics. The theoretical results provided support for the channel model of interaction proposed by Krebs and coworkers. According to this model, ThT binds in monomer form, into channels parallel to the fibril's long axis that are formed by amino acid side chains of the stacked β -sheets. Steric interactions between ThT and these side chains are considered responsible for the fluorescence enhancement of ThT upon binding. The Krebs model was also supported by computational results from Wolfe *et al.*^[209] who performed *ab initio* restricted Hartree-Fock calculations on ThT in interaction with an amyloid-like oligomer of β -2 microglobulin. Their results also revealed the preference of ThT monomers for channels formed by aromatic amino acids.

Nevertheless, as the X-ray diffraction data collected for the β -2 microglobulin oligomer revealed, dimer structures of ThT can also be encountered in the protein binding sites. Groenning *et al.* Groenning *et al.* Were the first to affirm the existence of amyloid-bound ThT dimers, on the basis of their molecular docking results corroborated with fluorescence and isothermal titration calorimetry data. They investigated the binding of ThT to β -sheet-rich (transthyretin, acetylcholinesterase) and non- β -sheet (β -, γ -cyclodextrins) cavities, observing that ThT binds to transthyretin and β -cyclodextrin in monomer form, and to acetylcholinesterase and γ -cyclodextrin as dimer (**Figure 8**). The latter interactions lead to a significant increase in fluorescence, with emission features similar to those observed in the presence of amyloid fibrils. The insight brought by Groenning's study was essential in understanding that not all β -sheet-rich structures have the ability to induce a significant fluorescence enhancement of ThT upon binding. In a recent report, Sulatskaya *et al.* Groen attention to the

existence of distinct emission profiles of the ThT excimer and of amyloid-bound ThT, after performing inner filter correction^[210] of the fluorescence spectra collected for a very broad range of ThT concentrations (3×10^{-6} M to 3×10^{-2} M), pointing out the danger of misinterpreting these two spectral signatures.

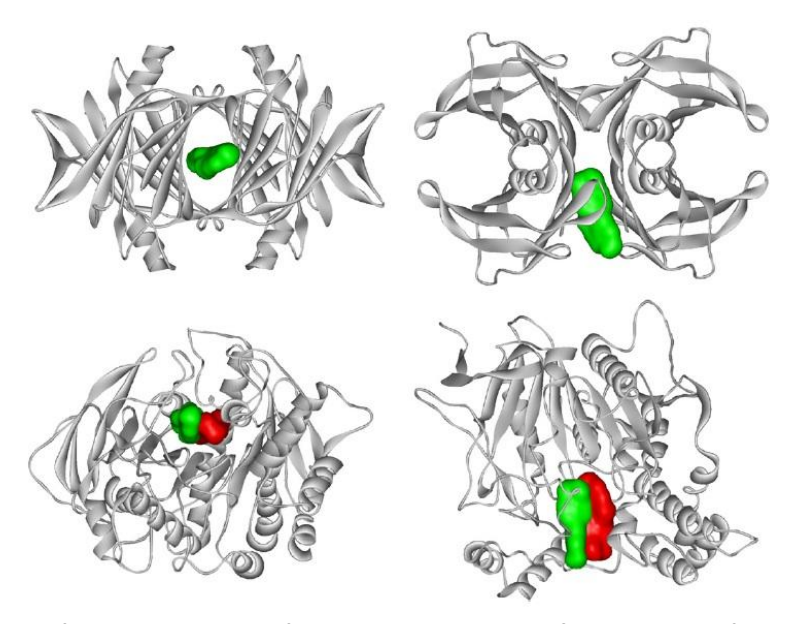


Figure 8. Energetically most favourable binding of ThT as monomer to the β-sheet cavity of transthyretin (upper) and as dimer to the cavity of acetylcholinesterase (lower). Reprinted from ref.^[171] J. Struct. Biol., 158/3, M. Groenning, L. Olsen, M. van de Weert, J. M. Flink, S. Frokjaer, F. S. Jorgensen, Study on the binding of Thioflavin T to beta-sheet-rich and non-beta-sheet cavities, 358–369, Copyright (2007), with permission from Elsevier; colour online.

The presence of amyloid-bound ThT dimers was also confirmed by Rodriguez-Rodriguez $et~al.^{[125]}$ in a study correlating X-ray diffraction data to DFT, molecular docking and molecular dynamics results. A neutral ThT derivative was also found to bind as dimer. More recently, Maskevich $et~al.^{[182]}$ performed geometry optimizations on ThT dimers using DFT calculations at the B3LYP/6-31G level. To construct the dimer structures, two relative arrangements of monomers were considered, namely head-to-head (H-aggregate, sandwich-type dimer) and in-line (J-aggregate, junction-type dimer). The H-aggregates with a small intermonomeric distance of 3.6 Å, in which intramolecular rotation around θ is not allowed, were found to be energetically favoured. Mudliar and Singh^[181] inferred that such H-aggregates may be responsible for the negative (+/-) Cotton effect observed in the ICD spectrum of ThT bound to heparin.

Molecular dynamics simulations performed by Zsila $et\ al.^{[63]}$ revealed that ThT binds to heparin as a $\pi-\pi$ stacked oligomer formed by up to six ThT dimers. This binding mode accounts for the blue shift of the absorption band via exciton coupling of the electronic transitions of ThT monomers, while the helical ordering of ThT oligomers along the chiral GAG chains is considered responsible for the exciton signals observed in the ICD spectrum (**Figure 5B**). The distance between monomers in the ThT dimer is 3.5–4 Å, and their arrangement is antiparallel, that is, the benzothiazole fragment of one monomer overlaps the benzyl moiety of the other. This energetically favoured dimer conformation can be explained by steric requirements imposed by the non-planar monomer geometries. Differently from the case of heparin, chondroitin 6-sulfate only interacts with one ThT dimer or trimer, and this can be corelated to the less significant changes observed in the absorption spectrum as compared to heparin. Most probably, this is due to the lower number of sulfate groups on this GAG, which prevents the formation of higher oligomers.

As discussed above, the peptide self-assembly mimic scaffolds^[175] represent another amyloid model system that captures the basic features of fibril-like β -sheet surfaces. They are of great utility for computational investigations, as they allow the researcher to operate targeted changes in the composition of amino acids, in order to gain insight into the minimal size requirements for ThT binding, and into the effects that aromaticity and attractive/repulsive electrostatic interactions have on the affinity of ThT for amyloids. A molecular dynamics study on these systems^[211] complemented the earlier experimental work (fluorescence and ICD).^[175] It is important to note that this study marks the first application of theoretical simulations to a well-defined binding site of ThT. Correlating the computational results with the experimental ones and making use of the available X-ray crystallographic data, several important conclusions have been drawn, as follows. ThT does not bind with high affinity to highly charged fibrils that have been designed to only possess charged side chains at the β -sheet surface. Instead, ThT favours the surface-exposed channels that are rich in hydrophobic, aromatic amino acids (tyrosine, phenylalanine, leucine). The primary binding site is represented by a groove formed by tyrosine and leucine residues adjacent on the β -sheet surface. Visualisation of this binding site (**Figure 9**) clearly evidences a dominant binding mode of ThT to aromatic residues across four consecutive β -strands, which was suggested as a generic recognition motif.

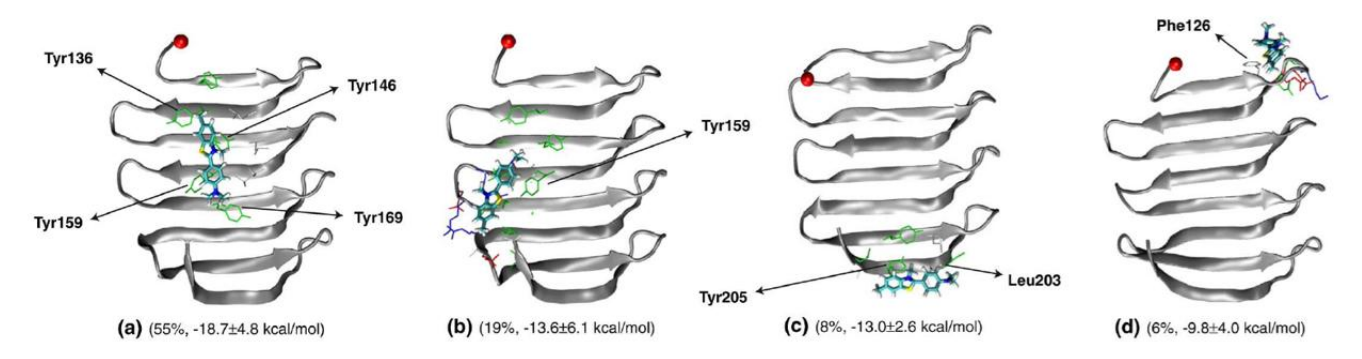


Figure 9. Binding modes of ThT to the single-layer β-sheet of the peptide self-assembly mimic 5-YY/LL: (a) on the top of five consecutive tyrosine side chains across β-strands; (b) on top of serine and threonine; (c) at the upper edge of the single-layer β-sheet; (d) at the lower edge of the single-layer β-sheet; abundances and MM-GBSA (molecular mechanics-generalized Born/surface area) binding energies in parentheses; N-terminus as red ball; surface side chains in blue (positively charged), red (negatively charged) and black (hydrophobic). Reprinted from ref.^[211] J. Mol. Biol., 394/4, C. Wu, M. Biancalana, S. Koide, J. E. Shea, Binding modes of thioflavin-T to the single-layer β-sheet of the peptide self-assembly mimics, 627–633, Copyright (2009), with permission from Elsevier; colour online.

Computational methods could contribute to the elucidation of the mechanism of amyloid disaggregation, thus facilitating the design of disaggregating agents with tailored characteristics. A combined molecular docking/molecular dynamics approach can be used, the former to examine the binding of the disaggregating agent to the amyloid fibril, and the latter to shed light into the molecular interactions leading to disaggregation. Umbrella Sampling calculations could also be of use in gaining an understanding of the molecular events leading to aggregation/disaggregation, and in identifying the formed intermediates. This computational technique was applied to the systems involving dimers of vanillin and methyl vanillate and albumins in order to monitor the displacement of the two ICD probes between proteins and to propose a dissociation pathway for each system. In the same study, DFT calculations at the B3LYP/6-31G(d) level were employed to simulate electronic circular dichroism spectra from individual spectra of minimum energy conformers, weighted by their respective Boltzmann population.

DFT calculations allowed to identify the origin of the bathochromic shift of the absorption band of ThT upon binding to insulin and to HET-s(218–289) amyloids.^[136] For this, *in vacuo* geometry optimizations at the B3LYP/6-31G(d) level were performed for the ThT monomer, for dimer structures constructed from coplanar

ThT monomers placed at different distances (16, 17, 18 Å) and in different relative mutual orientations (180–75 deg), and for ThT in interaction with a model β -sheet. This model of an amyloid structure consisted of five strands of triglycine capped with acetyl and methylamine groups mimicking the interaction of ThT with the polypeptide chain, as described previously. Single point TDDFT calculations were then performed at the B3LYP/6-31++G(d,p) level to simulate absorption spectra. It was found that both the dimer model and the interaction model account for the ~10 nm bathochromic shift in the absorption maximum of ThT. In the latter case, the minimum energy structure of the ground state complex suggests a parallel orientation of the dimethylaniline ring of ThT with respect to the peptide bond, with stabilization occurring via π - π stacking and dispersion interactions. Corroborating the DFT results with molecular dynamics data lalowed further exploration of the role played by the amino acid residues from the energetically favoured binding pockets in the preferential stabilization of ThT conformers with specific θ angle values. In the case of the dimer model, the positions and widths of the simulated and experimental absorption bands are in good agreement for an oblique arrangement of monomers situated at a distance of 17 Å and at a relative inclination of 120 deg. The authors note the presence of two exciton coupled states, and hint at the possibility that this dimer structure could give rise to the Cotton effects observed in the ICD spectrum in their previous study. In the case of the dimer structure could give rise to the Cotton effects observed in the ICD spectrum in their previous study.

Computational assessment of the interaction of ThT with native serum albumin was done by molecular docking in order to localize the binding pocket of ThT.^[165] Several conformers of ThT were predicted to bind to the binding site located in subdomain IB within a narrow free energy interval of 0.6 kcal/mol. In such a case, a concerted ICD/DFT analysis could pinpoint the preferred bound conformation, as we have previously demonstrated for several ligands belonging to the flavonoid class, for which the bound species (neutral, ^[54] anionic ^[55] or both ^[56]) and the bound conformations were successfully identified.

Coupling the experimental circular dichroism technique with quantum chemical calculations can provide valuable information on the number, identity and conformation of the bound species. This concerted approach is based on finding an identity between the experimental ICD spectrum and the theoretically computed electronic circular dichroism (ECD) spectrum. The method can be used in conjunction with molecular docking and molecular dynamics to confirm the results.^[55] More details on this facile approach, which can successfully substitute X-ray diffraction or NMR techniques in the quest to harness information on the bound molecule, can be found in ref.^[52] This perspective article was inspired by the results obtained in our group, and discusses the capabilities of the DFT method to predict the bound conformation of probes bearing in their structure one degree of freedom that becomes hindered upon interaction. In a recently published paper, we expanded this method to probes bearing two torsional degrees of freedom.^[58]

The first application of a concerted ICD/DFT approach to rationalize the features of ICD signals of ThT was reported by Dzwolak and Pecul. On the basis of DFT calculations at the B3LYP/6-311G(d,p) level of theory, the authors ascribed the strong negative ICD signal of ThT observed at 450 nm in the presence of insulin fibrils (**Figure 3A**) to the stabilisation of a bound ThT conformer having a positive θ value of +34.6 deg. This conformer is separated from its mirror image (θ = 145 deg = -35 deg) by a low energy barrier of 13.2 kJ/mol, which explains the lack of optical activity of free ThT in solution, through rapid interconversion. When ThT becomes entrapped by the fibril's chiral environment, intramolecular rotation about angle θ is hindered, and the sterically favoured chiral conformer prevails. As a general characteristic, ThT molecules with positive θ angle values exhibit negative ICD signals for the *homo-lumo* transition and, conversely, ThT conformers with negative θ values yield positive ICD signals, reflecting the opposite local chirality. θ

Once the X-ray structure of the complex of ThT with acetylcholinesterase became available, [213] it was revealed that ThT binds this enzyme as a planar conformer, in a microenvironment that is rich in aromatic amino acid side chains. The following major implication arose: any ICD signal observed for this complex cannot

be explained on the basis of intramolecular twisting and subsequent rigidization, but by a purely electronic mechanism. By using TDDFT calculations, Rybicka and Pecul^[214] conducted a theoretical study that has indeed demonstrated that the π - π interactions between ThT and the aromatic side chains of acetylcholinesterase are responsible for chirality induction. To ease the computational burden, the authors approximated the neighbouring tryptophan, tyrosine and phenylalanine aromatic amino acids from the X-ray structure of acetylcholinesterase by indole, phenol and toluene moieties, respectively (six aromatic rings in total, located at less than 4 Å from a planar ThT molecule, as shown in Figure 10). The rotatory strengths, responsible for the intensity of the ICD signal, were calculated in vacuo using the Coulomb-attenuated CAM-B3LYP functional, due to a consensus that this functional is superior to B3LYP for such calculations. The double-hybrid B2GPPLYP functional, much more computationally expensive, was also used, as it is generally recommended for systems exhibiting exciton coupling with aromatic chromophores. Both functionals were used in combination with the aug-cc-pVDZ atomic basis set. Additional calculations were performed using the IEE-PCM model with a dielectric constant of 4 in order to better mimic the hydrophobic protein microenvironment. It was shown that the degree of altering the electron density of ThT, as well as the coupling between electronic transitions of ThT and of the aromatic chromophores are determinant for the magnitude of the induced Cotton effect observed in the ECD spectrum (Figure 10). Importantly, the magnitude of this dichroic signal is comparable to that induced by a "chiral twist" mechanism. Through this investigation, the authors demonstrated for the first time that the presence of a chiral environment can contribute in a significant manner to the ICD of a planar ThT molecule. The main contribution originates in the tryptophan residue oriented parallel to the bound ThT molecule in the acetylcholinesterase binding pocket. The contribution from the crystallization water molecules was also considered, but found to be one order of magnitude smaller.

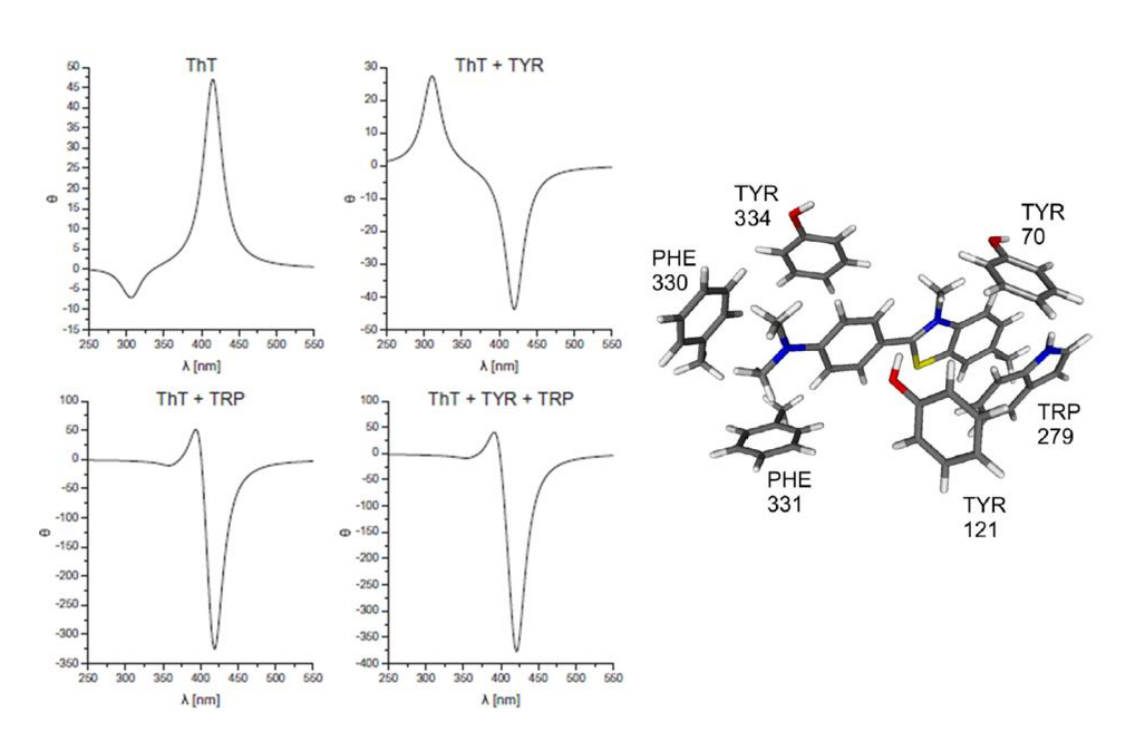


Figure 10. Left: *In vacuo* simulated ECD spectra of an isolated ThT molecule and of ThT in interaction with the aromatic rings of tyrosine (TYR), tryptophan (TRP) and both. Right: Aromatic rings mimicking the position of the amino acid side chains located at a distance of up to 4 Å from ThT in the acetylcholinesterase binding pocket. Reprinted from ref. [214] Chem. Phys., 463, A. Rybicka, M. Pecul, Induced circular dichroism of thioflavin T interacting with acetylcholinesterase: A computational study, 82–87, Copyright (2015), with permission from Elsevier; colour online.

The authors continued to explore the effect that the proximity of aromatic rings and other moieties like alkyl or polar side chains has on the ECD signal of ThT. [137] To eliminate the effect of the "chiral twist" mechanism, the value of angle θ was set to zero, and a benzene ring was placed successively in three distinct positions relative to the ThT molecule: above the phenyl ring of ThT (which resulted in a +ECD signal), above the $\sigma(C-C)$ bond connecting the two molecular fragments (+ECD signal) and above the benzothiazole moiety (-ECD signal). The benzene ring was placed at distances in the range 3–7 Å, and its orientation was varied from parallel (0 deg) to vertical (90 deg) in 15 deg increments. TDDFT calculations were then performed on these structures, without geometry optimization. The strongest +ECD signal (~40% of the one resulting from a "chiral twist" to a θ angle value of 30 deg) is obtained when the benzene ring is oriented parallel to the phenyl ring of ThT, and situated at a distance of 3 Å. Increasing the distance between the benzene ring and the ThT molecule determines a decrease in rotatory strength. The rotation of the benzene ring has little influence on the intensity of the ECD signal. The effect of the benzene ring is smaller than the one previously determined for a tryptophan moiety. [214] The dielectric constant of the environment was also varied (values of 4, 15, 78 were considered) to gain insight into the influence of polarity on the most stable ThT conformers in both So and S1 states. It was found that the dielectric constant has a more substantial influence on the equilibrium geometry of the S₁ state as compared to the S₀ state. In water (dielectric constant 78), the energetic minima correspond to θ angle values of 39.4 deg and 27.9 deg for S_0 and S_1 , respectively. To describe the folding of the two molecular fragments in ThT towards each other, the authors introduce a third, planar angle ξ having a value of ~177 deg in S₀, and ranging from 154.9 deg in vacuo to 163.2 deg in water, in S₁. On a separate note, the change in this bending angle upon excitation and upon binding to DNA was also investigated by other authors. [207,215] The value of dihedral angle ψ describing the internal rotation of the dimethylaniline fragment is not significantly influenced by the nature of the energy state (ground or excited) or by the polarity of the microenvironment, remaining in all cases at ~90 deg.

Not only the ICD spectral features, but also the circularly polarized luminescence spectra of ThT bound to insulin fibrils can be rationalized using TDDFT calculations. For this purpose, geometry optimization of ThT in the S_0 and S_1 states was performed at CAM-B3LYP/6-31+G(d) level, both *in vacuo* and using the IEE-PCM polarizable continuum model to simulate protein and aqueous environments. Potential energy surfaces in S_0 and S_1 states were constructed by varying angles θ and ψ , and the dependence of the rotatory and oscillator strengths on these torsion angles was analysed. The TDDFT spectral simulations were performed using the functional/basis set combinations CAM-B3LYP/6-31+G(d) and CAM-B3LYP/aug-cc-pVDZ. The results predicted that Cotton effects of the same order of magnitude are induced though the "chiral twist" mechanism and through electronic interactions with the protein aromatic rings in the close vicinity of ThT. As such, the authors concluded that the two mechanisms contribute to the same degree to the observed ICD and circularly polarized luminescence signals of ThT bound to insulin.

Concluding remarks and outlook

For over sixty years, ThT has been the main amyloid-specific dye used for examining the complex mechanisms responsible for protein aggregation and amyloid formation, by following its characteristic emissive signature. This review proposes a paradigm shift, bringing attention to applications of ThT that focus on chirality induction upon binding to amyloid fibrils. Upon closer examination, the induced circular dichroism of ThT, along with that of other amyloid-specific dyes, emerges as a valuable candidate for delving deeper into the complexity of amyloid systems. Among the spectroscopic techniques currently available, ICD stands out by

offering complementary insight to the widely used fluorescence spectroscopy, while being less affected by spectral bias from unbound species or from exogeneous compounds.

Until now, the characterization of amyloid systems by traditional high-resolution methods of structure determination like X-ray crystallography and solution NMR has been hindered by the inherent heterogeneity and poor solubility of the systems. In this context, assisting an accessible spectroscopic technique like ICD with computational methods (DFT, along with others) can provide otherwise unavailable structural information. The computational works overviewed here have revealed the great progress over recent years, in terms of computational cost of theoretical methods, which makes feasible investigations on increasingly complex systems.

Such a relatively fast and reliable approach to collect structural data is necessary in the context of the multitude of ThT derivatives currently being synthesized for *in vitro* and *in vivo* application, often through challenging routes, that require rapid screening of their spectral response and binding properties.

The concerted ICD/DFT approach may also serve to optimize current ThT assays with respect to several key aspects: identifying the conformation of the bound dye, the binding stoichiometry and kinetics, the degree to which the dye may influence fibril formation, the effect of competitive interactions with amyloid inhibitors. Findings from such studies may serve as guidelines for the design of new amyloid dyes and therapeutic amyloid inhibitors, and aid in the development of advanced detection methods. Working toward these goals, we hope that this review will encourage researchers to further document the potential of the ICD/DFT method, expanding the use of amyloid-specific dyes beyond their traditional fluorescence applications.

Acknowledgments

This work was supported by a grant of the Ministry of Research, Innovation and Digitization, CNCS-UEFISCDI, contract number 93TE/3.01.2025, project code PN-IV-P2-2.1-TE-2023-0189, within PNCDI IV. It was carried out within the research project "Nonuniform bio-binding" of the "Ilie Murgulescu" Institute of Physical Chemistry of the Romanian Academy.

Disclosure statement: The authors report there are no competing interests to declare.

References

- 1. G. Merlini, V. Bellotti, Molecular mechanisms of amyloidosis, N. Engl. J. Med. 349(6) (2003) 583–596. doi:10.1056/NEJMra023144
- 2. M. G. Iadanza, M. P. Jackson, E. W. Hewitt, N. A. Ranson, S. E. Radford, A new era for understanding amyloid structures and disease, Nat. Rev. Mol. Cell Biol. 19 (2018) 755–773. doi:10.1038/s41580-018-0060-8
- 3. D. Mehta, R. Jackson, G. Paul, J. Shi, M. Sabbagh, Why do trials for Alzheimer's disease drugs keep failing? A discontinued drug perspective for 2010–2015, Expert Opin. Investig. Drugs 26(6) (2017) 735–739. doi:10.1080/13543784.2017.1323868
- 4. F. Chiti, C. M. Dobson, Protein misfolding, functional amyloid, and human disease, Annu. Rev. Biochem. 75 (2006) 333–366. doi:10.1146/annurev.biochem.75.101304.123901

- 5. W. Dzwolak, A. Loksztejn, A. Galinska-Rakoczy, R. Adachi, Y. Goto and L. Rupnicki, J. Am. Chem. Soc. 129(24) (2007) 7517–7522. doi:10.1021/ja066703j
- 6. D. J. Lindberg, M. S. Wranne, M. Gilbert Gatty, F. Westerlund, E. K. Esbjörner, Steady-state and time-resolved Thioflavin-T fluorescence can report on morphological differences in amyloid fibrils formed by Ab(1-40) and Ab(1-42), Biochem. Biophys. Res. Commun. 458(2) (2015) 418–423. doi:10.1016/j.bbrc.2015.01.132
- 7. A. Precupas, R. Sandu, V. T. Popa, Quercetin influence on thermal denaturation of bovine serum albumin, J. Phys. Chem. B 120(35) (2016) 9362–9375. doi:10.1021/acs.jpcb.6b06214
- 8. A Precupas, A. R. Leonties, A. Neacsu, R. Sandu, V. T. Popa, Gallic acid influence on bovine serum albumin thermal stability, New J. Chem. 43 (2019) 3891–3898. doi:10.1039/C9NJ00115H
- 9. A. Precupas, V. T. Popa, Microcalorimetric investigation of ligand binding to BSA and its influence on the protein stability, in "Bovine Serum Albumin. Properties and Applications" (Ed. M. A. Masuelli), Nova Science Publisher, New York, USA, 2020, pp. 157–197.
- A. Precupas, R. Sandu, A. V. F. Neculae, A. Neacsu, V. T. Popa, Calorimetric, spectroscopic and computational investigation of morin binding effect on bovine serum albumin stability, J. Mol. Liq. 333 (2021) 115953. doi:10.1016/j.molliq.2021.115953
- 11. A. Precupas, A. R. Leonties, A. Neacsu, D. G. Angelescu, V. T. Popa, Bovine hemoglobin thermal stability in the presence of naringenin: Calorimetric, spectroscopic and molecular modeling studies, J. Mol. Liq. 361 (2022) 119617. doi:10.1016/j.molliq.2022.119617
- 12. A. Precupas, V. T. Popa, Impact of sinapic acid on bovine serum albumin thermal stability, Int. J. Mol. Sci. 25(2) (2024) 936. doi:10.3390/ijms25020936
- 13. A. Precupas, D. Gheorghe, A. R. Leonties, V. T. Popa, Resveratrol effect on α -lactalbumin thermal stability, Biomedicines 12(10) (2024) 2176. doi:10.3390/biomedicines12102176
- 14. A. Precupas, V. T. Popa, Insight into protein–ligand interaction: the effect on protein aggregation, in "Advances in Chemistry Research" (Ed. J. C. Taylor), volume 85, Nova Science Publisher, New York, USA, 2024, pp. 289–340.
- 15. M. R. H. Krebs, E. H. C. Bromley, A. M. Donald, The binding of thioflavin-T to amyloid fibrils: localization and implications, J. Struct. Biol. 149(1) (2005) 30–37. doi:10.1016/j.jsb.2004.08.002
- 16. N. Amdursky, Y. Erez, D. Huppert, Molecular rotors: What lies behind the high sensitivity of the thioflavin-T fluorescent marker, Acc. Chem. Res. 45(9) (2012) 1548–1557. doi:10.1021/ar300053p
- 17. M. Biancalana, S. Koide, Molecular mechanism of Thioflavin-T binding to amyloid fibrils, Biochim Biophys Acta. 2010, 1804(7), 1405–1412. doi:10.1016/j.bbapap.2010.04.001
- 18. A. A. Reinke, J. E. Gestwicki, Insight into amyloid structure using chemical probes, Chem. Biol. Drug Des. 77(6) (2011) 399–411. doi: 10.1111/j.1747-0285.2011.01110.x
- 19. A. C. Bhasikuttan, J. Mohanty, Detection, inhibition and disintegration of amyloid fibrils: Role of optical probes and macrocyclic receptors, Chem. Commun. 53 (2017) 2789–2809. doi:10.1039/C6CC08727B
- 20. K. G. Malmos, L. M. Blancas-Mejia, B. Weber, J. Buchner, M. Ramirez-Alvarado, H. Naiki, D. Otzen, ThT 101: a primer on the use of thioflavin T to investigate amyloid formation, Amyloid 24(1) (2017) 1–16. doi:10.1080/13506129.2017.1304905
- 21. R. Eisert, L. Felau, L. R. Brown, Methods for enhancing the accuracy and reproducibility of Congo red and thioflavin T assays, Anal. Biochem. 353(1) (2006) 144–146. doi:10.1016/j.ab.2006.03.015
- 22. Z. Zunbul, J. An, H. Aziz, J. Shin, S. Lim, L. Yu, Y. K. Kim, J. S. Kim, Tailoring hydrophobicity of Thioflavin T to optimize Aβ fibril bioimaging, Adv. NanoBiomed. Res. 3(6) (2023) 2200161. doi:10.1002/anbr.202200161

- 23. F. Yang, D. Yang, L. Wang, Q. Li, H. Zhang, L. Yao, H. Sun, Y. Tang, An inner salt derivative of Thioflavin T designed for live-cell imaging of mitochondrial G-quadruplexes, Sens. Actuators B. Chem. 374 (2023) 132820. doi:10.1016/j.snb.2022.132820
- 24. L. M. Needham, J. Weber, C. M. Pearson, D. T. Do, F. Gorka, G. Lyu, S. E. Bohndiek, T. N. Snaddon, S. F. Lee, A comparative photophysical study of structural modifications of Thioflavin T-inspired fluorophores, J. Phys. Chem. Lett. 11(19) (2020) 8406–8416. doi:10.1021/acs.jpclett.0c01549
- 25. V. I. Stsiapura, S. D. Gogoleva, A. A. Maskevich, O. V. Buganov, S. A. Tikhomirov, A. A. Lugovski, K. Baruah, B. K. Sarma, Effect of substituents on TICT rate in Thioflavin T-based fluorescent molecular rotors, Int. J. Nanosci. 18(03–04) (2019) 1940046. doi:10.1142/S0219581X19400465
- 26. A. Guan, X. F. Zhang, X. Sun, Q. Li, J. F. Xiang, L. X. Wang, L. Lan, F. M. Yang, S. J. Xu, X. M. Guo, Y. L. Tang, Ethyl-substitutive Thioflavin T as a highly-specific fluorescence probe for detecting G-quadruplex structure, Sci. Rep. 8 (2018) 2666. doi:10.1038/s41598-018-20960-7
- 27. K. Vus, V. Trusova, G. Gorbenko, R. Sood, P. Kinnunen, Thioflavin T derivatives for the characterization of insulin and lysozyme amyloid fibrils in vitro: Fluorescence and quantum-chemical studies, J. Lumin. 159 (2015) 284–293. doi: 10.1016/j.jlumin.2014.10.042
- 28. Y. Kataoka, H. Fujita, Y. Kasahara, T. Yoshihara, S.i Tobita, M. Kuwahara, Minimal Thioflavin T Modifications Improve Visual Discrimination of Guanine-Quadruplex Topologies and Alter Compound-Induced Topological Structures, Anal. Chem. 86(24) (2014) 12078–12084. doi:10.1021/ac5028325
- 29. W. E. Klunk, Y. Wang, G. F. Huang, M. L. Debnath, D. P. Holt, C. A. Mathis, Uncharged thioflavin-T derivatives bind to amyloid-beta protein with high affinity and readily enter the brain, Life Sci. 69(13) (2001) 1471–1484. doi:10.1016/S0024-3205(01)01232-2
- 30. C. A. Mathis, B. J. Bacskai, S. T. Kajdasz, M. E. McLellan, M. P. Frosch, B. T. Hyman, D. P. Holt, Y. Wang, G. F. Huang, M. L. Debnath, W. E. Klunk, A lipophilic thioflavin-T derivative for positron emission tomography (PET) imaging of amyloid in brain, Bioorg. Med. Chem. Lett. 12(3) (2002) 295–298. doi:10.1016/S0960-894X(01)00734-X
- 31. A. Lockhart, L. Ye, D. B. Judd, A. T. Merritt, P. N. Lowe, Evidence for the presence of three distinct binding sites for the thioflavin T class of Alzheimer's disease PET imaging agents on β-amyloid peptide fibrils, 280(9) (2005) 7677–7684. doi:10.1074/jbc.M412056200
- 32. L. Cai, R. B. Innis, V. W. Pike, Radioligand development for PET imaging of β -Amyloid (A β)-current status, Curr. Med. Chem. 14(1) (2007) 19–52. doi:10.2174/092986707779313471
- 33. C. A. Mathis, N. S. Mason, B. J. Lopresti, W. E. Klunk, Development of positron emission tomography β-amyloid plaque imaging agents, Semin. Nucl. Med. 42(6) (2012) 423–432. doi:10.1053/j.semnuclmed.2012.07.001
- 34. S. Alavez, M. C. Vantipalli, D. J. S. Zucker, I. M. Klang, G. J. Lithgow, Amyloid-binding compounds maintain protein homeostasis during ageing and extend lifespan, Nature 472(7342) (2011) 226–229. doi:10.1038/nature09873
- 35. W. E. Klunk, H. Engler, A. Nordberg, Y. Wang, G. Blomqvist, D. P. Holt, M. Bergström, I. Savitcheva, G. F. Huang, S. Estrada, B. Ausén, M. L. Debnath, J. Barletta, J. C. Price, J. Sandell, B. J. Lopresti, A. Wall, P. Koivisto, G. Antoni, C. A. Mathis, B. Långström, Imaging brain amyloid in Alzheimer's disease with Pittsburgh Compound-B, Ann. Neurol. 55(3) (2004) 306–319. doi:10.1002/ana.20009
- 36. S. Anselmo, G. Sancataldo, V. Vetri, Deciphering amyloid fibril molecular maturation through FLIM-phasor analysis of thioflavin T, Biophys. Rep. 4(1) (2024) 100145. doi:10.1016/j.bpr.2024.100145
- 37. Q. Yang, E. Hosseini, P. Yao, S. Pütz, M. Gelléri, M. Bonn, S. H. Parekh, X. Liu, Self-blinking Thioflavin T for super-resolution imaging, J. Phys. Chem. Lett. 15(30) (2024) 7591–7596. doi:10.1021/acs.jpclett.4c00195

- 38. J. Q. Du, W. C. Luo, J. T. Zhang, Q. Y. Li, L. N. Bao, M. Jiang, X. Yu, L. Xu, Machine learning-assisted fluorescence/fluorescence colorimetric sensor array for discriminating amyloid fibrils, Sens. Actuators B. Chem. 417 (2024) 136173. doi:10.1016/j.snb.2024.136173
- 39. B. Halder, S. Ghosh, T. Khan, S. Pal, N. Das, P. Sen, Tracking heterogenous protein aggregation at nanoscale through fluorescence correlation spectroscopy, Photochem. Photobiol. 100(4) (2024) 989–999. doi:10.1111/php.14004
- 40. K. Rusakov, A. El-Turabi, L. Reimer, P. H. Jensen, P. Hanczyc, Thioflavin T a reporter of microviscosity in protein aggregation process: The study case of α-synuclein, J. Phys. Chem. Lett. 15(25) (2024) 6685–6690. doi:10.1021/acs.jpclett.4c00699
- 41. A. Sarkar, V. Namboodiri, M. Kumbhakar, Fluorescence correlation spectroscopy measurements on amyloid fibril reveal at least two binding modes for fluorescent sensors, Chem. Phys. Impact 7 (2023) 100369. doi:10.1016/j.chphi.2023.100369
- 42. M. Sunder, N. Acharya, S. Nayak, N. Mazumder, Optical spectroscopy and microscopy techniques for assessment of neurological diseases, Appl. Spectrosc. Rev. 56(8-10) (2021) 764–803. doi:10.1080/05704928.2020.1851237
- 43. I. Matei, A. M. Ariciu, M. V. Neacsu, A. Collauto, A. Salifoglou, G. Ionita, Cationic spin probe reporting on thermal denaturation and complexation-decomplexation of BSA with SDS. Potential applications in protein purification processes, J. Phys. Chem. B 118(38) (2014) 11238–11252. doi:10.1021/jp5071055
- 44. S. Mocanu, I. Matei, S. Ionescu, V. Tecuceanu, G. Marinescu, P. Ionita, D. Culita, A. Leonties, G. Ionita, Complexation of β-cyclodextrin with dual molecular probes bearing fluorescent and paramagnetic moieties linked by short polyether chains, Phys. Chem. Chem. Phys. 19 (2017) 27839–27847. doi:10.1039/C7CP05276F
- 45. S. Mocanu, G. Ionita, S. Ionescu, V. Tecuceanu, M. Enache, A. R. Leonties, C. Stavarache, I. Matei, New environment-sensitive bis-dansyl molecular probes bearing alkyl diamine linkers: Emissive features and interaction with cyclodextrins, Chem. Phys. Lett. 713 (2018) 226–234. doi:10.1016/j.cplett.2018.10.044
- 46. R. Baratoiu, S. Mocanu, I. Matei, M. Bem, E. Hristea, V. Tecuceanu, G. Ionita, A comparison of the behavior of monomolecular and dual molecular probes in F127/cyclodextrin systems, Macromol. Chem. Phys. 220(5) (2019) 1800489. doi:10.1002/macp.201800489
- 47. S. Mocanu, I. Matei, A. Leonties, V. Tecuceanu, A. Hanganu, Z. Minea, A. Stancu, E. I. Popescu, G. Ionita, "New flexible molecular probes bearing dansyl and tempo moieties for host–guest interactions in solution and gels, New J. Chem. 43 (2019) 11233–11240. doi:10.1039/C9NJ01554J
- 48. S. Mocanu, G. Ionita, I. Matei, Solvatochromic characteristics of dansyl molecular probes bearing alkyl diamine chains, Spectrochim. Acta A Mol. Biomol. Spectrosc. 237 (2020) 118413. doi:10.1016/j.saa.2020.118413
- 49. I. Matei, A. M. Ariciu, E. I. Popescu, S. Mocanu, A. V. F. Neculae, F. Savonea, G. Ionita, Evaluation of the accessibility of molecules in hydrogels using a scale of spin probes, Gels 8(7) (2022) 428. doi:10.3390/gels8070428
- 50. A. V. F. Neculae, G. Audran, S. Bourdillon, G. Ionita, J. P. Joly, S. R. A. Marque, I. Matei, S. Mocanu, Conformational changes in β-phosphorylated nitroxides a powerful tool to probe host–guest interactions, J. Mol. Liq. 364 (2022) 119983. doi:10.1016/j.molliq.2022.119983
- 51. D. G. Angelescu, G. Ionita, Evaluation of all-atom and Martini 3 coarse-grained force fields from the structural investigation of nitroxide spin probes and their confinement in beta-cyclodextrin, J. Phys. Chem. B 128(47) (2024) 11784–11799. doi:10.1021/acs.jpcb.4c04970
- 52. S. Ionescu, I. Matei, C. Tablet, M. Hillebrand, Theoretical ECD calculations A useful tool in estimating the conformational change of a ligand in the binding pocket of proteins, Phys. Chem. Chem. Phys. 15 (2013) 11604–11614. doi:10.1039/c3cp50466b

- 53. S. Ionescu, I. Matei, C. Tablet, M. Hillebrand, New insights on flavonoid-serum albumin interactions from concerted spectroscopic methods and molecular modeling, Curr. Drug Metab. 14(4) (2013) 474–490. doi:10.2174/1389200211314040010
- 54. I. Matei, S. Ionescu, M. Hillebrand, Induced chirality of genistein upon binding to albumin: circular dichroism and TDDFT study, Rev. Roum. Chim. 58(4–5) (2013) 409–413.
- 55. I. Matei, S. Ionescu, M. Hillebrand, Kaempferol–human serum albumin interaction: Characterization of the induced chirality upon binding by experimental circular dichroism and TDDFT calculations, Spectrochim. Acta A Mol. Biomol. Spectrosc., 96 (2012) 709–715. doi:10.1016/j.saa.2012.07.043
- 56. I. Matei, S. Ionescu, M. Hillebrand, Induced chirality in fisetin upon binding to serum albumin: experimental circular dichroism and TDDFT calculations, J. Mol. Model. 18 (2012) 4381–4387. doi:10.1007/s00894-012-1444-x
- 57. A. Varlan, M. Hillebrand, Exploring the capabilities of TDDFT calculations to explain the induced chirality upon a binding process: A simple case, 3-carboxycoumarin, J. Mol. Struct. 1036 (2013) 341–349. doi:10.1016/j.molstruc.2012.11.060
- 58. C. Tablet, I. Matei, S. Ionescu, M. Hillebrand, Experimental and theoretical ECD study of the 7-methoxycoumarin-3-carboxylic acid binding to BSA", Rev. Roum. Chim. 69(5-6) (2024) 247–253. doi:10.33224/rrch.2024.69.5-6.02
- 59. S. Sharma, S. Deep, Inhibition of fibril formation by polyphenols: molecular mechanisms, challenges, and prospective solutions, Chem. Commun. 60 (2024) 6717–6727. doi:10.1039/D4CC00822G
- 60. H. Parvej, S. Begum, R. Dalui, S. Paul, B. Mondal, S. Sardar, N. Sepay, G. Maiti, U. C. Halder, Coumarin derivatives inhibit the aggregation of β-lactoglobulin, RSC Adv. 12 (2022) 17020–17028. doi:10.1039/d2ra01029a
- 61. M. S. Nair, Spectroscopic studies on the interaction of serum albumins with plant derived natural molecules, Appl. Spectrosc. Rev. 53(8) (2017) 636–666. doi:10.1080/05704928.2017.1402184
- 62. W. Dzwolak, M. Pecul, Chiral bias of amyloid fibrils revealed by the twisted conformation of Thioflavin T: An induced circular dichroism/DFT study, FEBS Letters 579(29) (2005) 6601–6603. doi:10.1016/j.febslet.2005.10.048
- 63. F. Zsila, S. A. Samsonov, M. Maszota-Zieleniak, Mind your dye: The amyloid sensor Thioflavin T interacts with sulfated glycosaminoglycans used to induce cross-β-sheet motifs, J. Phys. Chem. B 124(51) (2020) 11625–11633. doi:10.1021/acs.jpcb.0c08273
- 64. V. Babenko, W. Dzwolak, Thioflavin T forms a non-fluorescent complex with a-helical poly-L-glutamic acid, Chem. Commun., 2011, 47, 10686–10688. doi:10.1039/C1CC14230E
- 65. N. R. Rovnyagina, T. N. Tikhonova, V. O. Kompanets, N. N. Sluchanko, K. V. Tugaeva, S. V. Chekalin, V. V. Fadeev, J. Lademann, M. E. Darvin, E. A. Shirshin, Free and bound thioflavin T molecules with ultrafast relaxation: implications for assessment of protein binding and aggregation, Laser Phys. Lett. 16 (2019) 075601. doi:10.1088/1612-202X/ab2244
- 66. E. Coelho-Cerqueira, A. S. Pinheiro, C. Follmer, Pitfalls associated with the use of Thioflavin-T to monitor anti-fibrillogenic activity, Bioorg. Med. Chem. Lett. 24(14) (2014) 3194–3198. doi:10.1016/j.bmcl.2014.04.072
- 67. M. Sebastiao, N. Quittot, S. Bourgault, Thioflavin T fluorescence to analyse amyloid formation kinetics: Measurement frequency as a factor explaining irreproducibility, Anal. Biochem. 532 (2017) 83–86. doi:10.1016/j.ab.2017.06.007
- 68. D. J. Lindberg, A. Wenger, E. Sundin, E. Wesén, F. Westerlund, E. K. Esbjörner, Binding of Thioflavin-T to amyloid fibrils leads to fluorescence self-quenching and fibril compaction, Biochemistry 56(16) (2017) 2170–2174. doi:10.1021/acs.biochem.7b00035

- 69. S. A. Hudson, H. Ecroyd, T. W. Kee, J. A. Carver, The thioflavin T fluorescence assay for amyloid fibril detection can be biased by the presence of exogenous compounds, FEBS J. 276(20) (2009) 5960–5972. doi:10.1111/j.1742-4658.2009.07307.x
- 70. Y. Porat, A. Abramowitz, E. Gazit, Inhibition of amyloid fibril formation by polyphenols: structural similarity and aromatic interactions as a common inhibition mechanism, Chem. Biol. Drug. Des. 67(1) (2006) 27–37. doi:10.1111/j.1747-0285.2005.00318.x
- 71. A. K. Buell, C. M. Dobson, T. P. J. Knowles, M.E. Welland, Interactions between amyloidophilic dyes and their relevance to studies of amyloid inhibitors, Biophys. J. 99(10) (2010) 3492–3497. doi:10.1016/j.bpj.2010.08.074
- 72. M. Ziaunys, K. Mikalauskaite, V. Smirnovas, Amyloidophilic molecule interactions on the surface of insulin fibrils: Cooperative binding and fluorescence quenching, Sci. Rep. 9 (2019) 20303. doi:10.1038/s41598-019-56788-y
- 73. A. Noormägi, K. Primar, V. Tõugua, P. Palumaa, Interference of low-molecular substances with the thioflavin-T fluorescence assay of amyloid fibrils, J. Pept. Sci. 18(1) (2012) 59–64. doi:10.1002/psc.1416
- 74. F. Meng, P. Marek, K. J. Potter, C. B. Verchere, D. P. Raleigh, Rifampicin does not prevent amyloid fibril formation by human islet amyloid polypeptide but does inhibit fibril thioflavin-T interactions: implications for mechanistic studies of beta-cell death, Biochemistry 47(22) (2008) 6016–6024. doi:10.1021/bi702518m
- 75. J. Ryu, M. Kanapathipillai, G. Lentzen, C. B. Park, Inhibition of beta-amyloid peptide aggregation and neurotoxicity by alpha-d-mannosylglycerate, a natural extremolyte, Peptides 29(4) (2008) 578–584. doi:10.1016/j.peptides.2007.12.014
- 76. E. V. Hackl, J. Darkwah, G. Smith, I. Ermolina, Effect of acidic and basic pH on Thioflavin T absorbance and fluorescence, Eur. Biophys. J. 44 (2015) 249–261. doi:10.1007/s00249-015-1019-8
- 77. E. Arad, H. Green, R. Jelinek, H. Rapaport, Revisiting thioflavin T (ThT) fluorescence as a marker of protein fibrillation The prominent role of electrostatic interactions, J. Coll. Interf. Sci. 573 (2020) 87–95. doi:10.1016/j.jcis.2020.03.075
- 78. R. Sabaté, I. Lascu, S. J. Saupe, On the binding of Thioflavin-T to HET-s amyloid fibrils assembled at pH 2, J. Struct. Biol. 162(3) (2008) 387–396. doi:10.1016/j.jsb.2008.02.002
- 79. H. Naiki, K. Higuchi, M. Hosokawa, T. Takeda, Fluorometric determination of amyloid fibrils in vitro using the fluorescent dye, thioflavin T1, Anal. Biochem. 177(2) (1989) 244–249. doi:10.1016/0003-2697(89)90046-8
- 80. H. LeVine III, Thioflavine T interaction with synthetic Alzheimer's disease beta-amyloid peptides: detection of amyloid aggregation in solution, Protein Sci. 2(3) (1993) 404–410. doi:10.1002/pro.5560020312
- 81. P. S. Vassar, C. F. Culling, Fluorescent stains, with special reference to amyloid and connective tissues, Arch. Pathol. 68 (1959) 487–498.
- 82. E. S. Voropai, Spectral properties of Thioflavin T and its complexes with amyloid fibrils, J. Appl. Spectrosc. 70 (2003) 868–874. doi:10.1023/B:JAPS.0000016303.37573.7e
- 83. L. R. Naika, A. B. Naika, H. Pal, Steady-state and time-resolved emission studies of Thioflavin-T, J. Photochem. Photobiol. A Chem. 204(2–3) (2009) 161–167. doi:10.1016/j.jphotochem.2009.03.016
- 84. V. I. Stsiapura, S. A. Kurhuzenkau, V. A. Kuzmitsky, O. V. Bouganov, S. A. Tikhomirov, Solvent polarity effect on nonradiative decay rate of Thioflavin T, J. Phys. Chem. A 120(28) (2016) 5481–5496. doi:10.1021/acs.jpca.6b02577
- 85. S. Freire, M. H. de Araujo, W. Al-Soufi, M. Novo, Photophysical study of Thioflavin T as fluorescence marker of amyloid fibrils, Dyes Pigm. 2014, 110, 97–105. doi:10.1016/j.dyepig.2014.05.004

- 86. V. I. Stsiapura, A. A. Maskevich, V. A. Kuzmitsky, V. N. Uverskylrina, I. M. Kuznetsova, K. K. Turoverov, Thioflavin T as a molecular rotor: fluorescent properties of Thioflavin T in solvents with different viscosity, J. Phys. Chem. B 112(49) (2008) 15893–15902. doi:10.1021/jp805822c
- 87. V. I. Stsiapura, A. A. Maskevich, S. A. Tikhomirov, O. V. Buganov, Charge transfer process determines ultrafast excited state deactivation of thioflavin T in low-viscosity solvents, J. Phys. Chem. A 114(32) (2010) 8345–8350. doi:10.1021/jp105186z
- 88. P. K. Singh, M. Kumbhakar, H. Pal, S. Nath, Viscosity effect on the ultrafast bond twisting dynamics in an amyloid fibril sensor: Thioflavin-T, J. Phys. Chem. B 114(17) (2010) 5920–5927. doi:10.1021/jp100371s
- 89. V. Fodera, M. Groenning, V. Vetri, F. Librizzi, S. Spagnolo, C. Cornett, L. Olsen, M. van de Weert, M. Leone, Thioflavin T hydroxylation at basic ph and its effect on amyloid fibril detection, J. Phys. Chem. B 112(47) (2008) 15174–15181. doi:10.1021/jp805560c
- 90. A. Chatterjee, B. Maity, D. Seth, Torsional dynamics of thioflavin T in room-temperature ionic liquids: An effect of heterogeneity of the medium, ChemPhysChem 14(14) (2013) 3400–3409. doi:10.1002/cphc.201300433
- 91. P. K. Singh, A. K. Mora, S. Nath, Ultrafast torsional relaxation of thioflavin-T in tris(pentafluoroethyl)trifluorophosphate (fap) anion-based ionic liquids, J. Phys. Chem. B 119(44) (2015) 14252–14260. doi:10.1021/acs.jpcb.5b09028
- 92. R. K. Gautam, S. A. Ahmed, D. Seth, Photophysics of Thioflavin T in deep eutectic solvents, J. Lumin. 198 (2018) 508–516. doi:10.1016/j.jlumin.2018.02.055
- 93. P. K. Singh, M. Kumbhakar, H. Pal, S. Nath, Confined ultrafast torsional dynamics of Thioflavin-T in a nanocavity, Phys. Chem. Chem. Phys. 13 (2011) 8008–8014. doi:10.1039/C0CP02635B
- 94. C. Retna Raj, R. Ramaraj, Influence of cyclodextrin complexation on the emission of thioflavin T and its off-on control, J. Photochem. Photobiol. A Chem. 122(1) (1999) 39–46. doi:10.1016/S1010-6030(99)00004-0
- 95. A. A. Maskevich, S. A. Kurhuzenkau, A. Yu. Lickevich, Fluorescence spectral analysis of thioflavin T–γ-cyclodextrin interaction, J. Appl. Spectrosc. 80 (2013) 36–42. doi:10.1007/s10812-013-9717-4
- 96. G. Singh, S. P. Pandey, P. K. Singh, Guest binding with sulfated cyclodextrins: Does the size of cavity matter? ChemPhysChem 24(4) (2023) e202200421. doi:10.1002/cphc.202200421
- 97. A. C. Bhasikuttan, S. D. Choudhury, H. Pal, J. Mohanty, Supramolecular assemblies of Thioflavin T with cucurbiturils: Prospects of cooperative and competitive metal ion binding, Isr. J. Chem. 51(5–6) (2011) 634–645. doi:10.1002/ijch.201100039
- 98. C. Saravanan, B. C. M. Arputham Ashwin, M. Senthilkumaran, P. M. Mareeswaran, Supramolecular complexation of biologically important thioflavin-T with p-sulfonatocalix[4]arene, ChemistrySelect 3(9) (2018) 2528–2535. doi:10.1002/slct.201702937
- 99. S. Kumar, A. K. Singh, G. Krishnamoorthy, R. Swaminathan, Thioflavin T displays enhanced fluorescence selectively inside anionic micelles and mammalian cells, J. Fluoresc. 18 (2008) 1199–1205. doi:10.1007/s10895-008-0378-2
- 100. P. K. Singh, M. Kumbhakar, H. Pal, S. Nath, A nano-confined charged layer defies the principle of electrostatic interaction, Chem. Commun. 47 (2011) 6912–6914. doi:10.1039/c1cc10881f
- 101. I. A. Heisler, S. R. Meech, Altered relaxation dynamics of excited state reactions by confinement in reverse micelles probed by ultrafast fluorescence up-conversion, Chem. Soc. Rev 50 (2021) 11486. doi:10.1039/d1cs00516b

- 102. J. P. Leite, L. Gales, Fluorescence properties of the amyloid indicator dye thioflavin T in constrained environments, Dyes Pigm. 160 (2019) 64–70. doi:10.1016/j.dyepig.2018.07.049
- 103. R. Hazra, N. Bera, S. Layek, N. Sarkar, Efficiency of encapsulation of thioflavin T (ThT) into polar and nonpolar environments of different bile salt aggregates: A femtosecond fluorescence study, Langmuir 40(31) (2024) 16272–16282. doi:10.1021/acs.langmuir.4c01460
- 104. S. Murudkar, A. K. Mora, P. K. Singh, S. Nath, Ultrafast molecular rotor: an efficient sensor for premelting of natural DNA, Chem. Commun. 48 (2012) 5301–5303. doi=10.1039/C2CC30895A
- 105. P. K. Singh, S. Nath, Molecular recognition controlled delivery of a small molecule from a nanocarrier to natural DNA, J. Phys. Chem. B 117(36) (2013) 10370–10375. doi:10.1021/jp402902k
- 106. J. Mohanty, N. Barooah, V. Dhamodharan, S. Harikrishna, P. I. Pradeepkumar, A. C. Bhasikuttan, Thioflavin T as an efficient inducer and selective fluorescent sensor for the human telomeric G-quadruplex DNA, J. Am. Chem. Soc. 135(1) (2013) 367–376. doi:10.1021/ja309588h
- 107. P. Hanczyc, Role of alkali cations in DNA-thioflavin T interaction, J. Phys. Chem. B 128(31) (2024) 7520–7529. doi:10.1021/acs.jpcb.4c02417
- 108. L. Jiang, J. Teng, X. Liu, L. Xu, T. Yang, X. Hu, S. Ding, J. Li, Y. Jiang, W. Cheng, Interaction analysis of RNA G-quadruplex with ligands and in situ imaging application, Anal. Biochem. 694 (2024) 115613. doi:10.1016/j.ab.2024.115613
- 109. P. Hanczyc, P. Rajchel-Mieldzioć, B. Feng, P. Fita, Identification of thioflavin T binding modes to DNA: A structure-specific molecular probe for lasing applications, J. Phys. Chem. Lett. 12(22) (2021) 5436–5442. doi:10.1021/acs.jpclett.1c01254
- 110. P. Kumaraswamy, R. Lakshmanan, S. Sethuraman, U. M. Krishnan, Self-assembly of peptides: influence of substrate, pH and medium on the formation of supramolecular assemblies, Soft Matter 7 (2011) 2744–2754. doi:10.1039/c0sm00897d
- 111. S. Sarma, T. R. Sudarshan, V. Nguyen, A. S. Robang, X. Xiao, J. V. Le, M. E. Helmicki, A. K. Paravastu, C. K. Hall, Design of parallel β-sheet nanofibrils using Monte Carlo search, coarse-grained simulations, and experimental testing, Protein Sci. 33(8) (2024) e5102. doi:10.1002/pro.5102
- 112. A. Adak, V. Castelletto, B. Mendes, G. Barrett, J. Seitsonen, I. W. Hamley, Chirality and pH influence the self-assembly of antimicrobial lipopeptides with diverse nanostructures, ACS Appl. Bio Mater. 7(8) (2024) 5553–5565. doi:10.1021/acsabm.4c00664
- 113. F. Zsila, H. Matsunaga, Z. Bikádi, J. Haginaka, Multiple ligand-binding properties of the lipocalin member chicken α_1 -acid glycoprotein studied by circular dichroism and electronic absorption spectroscopy: The essential role of the conserved tryptophan residue, Biochim. Biophys. Acta 1760(8) (2006) 1248–1273. doi:10.1016/j.bbagen.2006.04.006
- 114. P. Sen, S. Fatima, B. Ahmad, R. H. Khan, Interactions of thioflavin T with serum albumins: spectroscopic analyses, Spectrochim. Acta A Mol. Biomol. Spectrosc. 74(1) (2009) 94–99. doi:10.1016/j.saa.2009.05.010
- 115. A. I. Sulatskaya, G. N. Rychkov, M. I. Sulatsky, N. P. Rodina, I. M. Kuznetsova, K. K. Turoverov, Thioflavin T interaction with acetylcholinesterase: New evidence of 1:1 binding stoichiometry obtained with samples prepared by equilibrium microdialysis, ACS Chem. Neurosci. 9(7) (2018) 1793–1801. doi:10.1021/acschemneuro.8b00111
- 116. P. K. Singh, A. K. Mora, S. Nath, Ultrafast fluorescence spectroscopy reveals a dominant weakly-emissive population of fibril bound Thioflavin-T, Chem. Commun. 51 (2015) 14042–14045. doi:10.1039/C5CC04256A

- 117. A. I. Sulatskaya, A. V. Lavysh, A. A. Maskevich, I. M. Kuznetsova, K. K. Turoverov, Thioflavin T fluoresces as excimer in highly concentrated aqueous solutions and as monomer being incorporated in amyloid fibrils, Sci. Rep. 7 (2017) 2146. doi:10.1038/s41598-017-02237-7
- 118. V. Trusova, U. Tarabara, O. Zhytniakivska, K. Vus, G. Gorbenko, Förster resonance energy transfer analysis of amyloid state of proteins, BBA Advances 2 (2022) 100059. doi:10.1016/j.bbadva.2022.100059
- 119. J. Raeburn, L. Chen, S. Awhida, R. C. Deller, M. Vatish, M. I. Gibson, D. J. Adams, Using molecular rotors to probe gelation, Soft Matter 11 (2015) 3706–3713. doi:10.1039/c5sm00456j
- 120. G. Giovannini, P. Cinelli, L. F. Boesel, R. M. Rossi, Thioflavin-modified molecularly imprinted hydrogel for fluorescent-based non-enzymatic glucose detection in wound exudate, Mater. Today Bio 14 (2022) 100258. doi:10.1016/j.mtbio.2022.100258
- 121. S. Bhowmik, B. Baral, T. Rit, H. C. Jha, A. K. Das, Design and synthesis of a nucleobase functionalized peptide hydrogel: in vitro assessment of anti-inflammatory and wound healing effects, Nanoscale 16 (2024) 13613–13626. doi:10.1039/D4NR01149J
- 122. V. I. Stsiapura, A. A. Maskevich, V. A. Kuzmitsky, K. K. Turoverov, I. M. Kuznetsova, Computational study of thioflavin T torsional relaxation in the excited state, J. Phys. Chem. A 111(22) (2007) 4829–4835. doi:10.1021/jp0705900
- 123. A. A. Maskevich, V. I. Stsiapura, V. A. Kuzmitsky, I. M. Kuznetsova, O. I. Povarova, V. N. Uversky and K. K. Turoverov, J. Proteome Res. 6(4) (2007) 1392–1401. doi:10.1021/pr0605567
- 124. M. A. Haidekker, M. Nipper, A. Mustafic, D. Lichlyter, M. Dakanali, E. A. Theodorakis, Dyes with Segmental Mobility: Molecular Rotors, in Advanced Fluorescence Reporters in Chemistry and Biology I. Fundamentals and Molecular Design, ed. A. P. Demchenko, Springer-Verlag, Berlin, 2010, vol. I, pp. 267–308.
- 125. C. Rodriguez-Rodriguez, A. Rimola, L. Rodriguez-Santiago, P. Ugliengo, A. Alvarez-Larena, H. Gutierrez-de-Teran, M. Sodupe, P. Gonzalez-Duarte, Crystal structure of thioflavin-T and its binding to amyloid fibrils: insights at the molecular level, Chem. Commun. 46 (2010) 1156–1158. doi:10.1039/b912396b
- 126. M. A. Haidekker, E. A. Theodorakis, Molecular rotors fluorescent biosensors for viscosity and flow, Org. Biomol. Chem. 5 (2007) 1669–1678. doi:10.1039/B618415D
- 127. P. K. Singh, M. Kumbhakar, H. Pal, S. Nath, Ultrafast bond twisting dynamics in amyloid fibril sensor, J. Phys. Chem. B 114(7) (2010) 2541–2546. doi:10.1021/jp911544r
- 128. A. Srivastava, P. K. Singh, M. Kumbhakar, T. Mukherjee, S. Chattopadyay, H. Pal, S. Nath, Identifying the bond responsible for the fluorescence modulation in an amyloid fibril sensor, Chem. Eur. J. 16(30) (2010) 9257–9263. doi:10.1002/chem.200902968
- 129. P. Mukherjee, S. Rafiq, P. Sen, Dual relaxation channel in thioflavin-T: An ultrafast spectroscopic study, J. Photochem. Photobiol. A Chem. 328 (2016) 136–147. doi:10.1016/j.jphotochem.2016.05.012
- 130. P. Mukherjee, A. Das, P. Sen, Ultrafast excited state deactivation channel of thioflavin T adsorbed on SDS micelle: A combined femtosecond fluorescence and transient absorption study, J. Photochem. Photobiol. A Chem. 348 (2017) 287–294. doi:10.1016/j.jphotochem.2017.08.059
- 131. A. I. Sulatskaya, A. A. Maskevich, I. M. Kuznetsova, V. N. Uversky, K. K. Turoverov, Fluorescence quantum yield of thioflavin T in rigid isotropic solution and incorporated into the amyloid fibrils, PLoS ONE 5 (2010) e15385. doi:10.1371/journal.pone.0015385
- 132. P. K. Singh, M. Kumbhakar, H. Pal, S. Nath, Ultrafast Torsional Dynamics of Protein Binding Dye Thioflavin-T in Nanoconfined Water Pool, J. Phys. Chem. B 113(25) (2009) 8532–8538. doi:10.1021/jp902207k

- 133. I. M. Kuznetsova, A. I. Sulatskaya, A. A. Maskevich, V. N. Uversky, K. K. Turoverov, High fluorescence anisotropy of thioflavin T in aqueous solution resulting from its molecular rotor nature, Anal. Chem. 88(1) (2016) 718–724. doi:10.1021/acs.analchem.5b02747
- 134. J. C. K. Kung, N. Vurgun, J. C. Chen, M. Nitz, R. A. Jockusch, Intrinsic turn-on response of thioflavin T in complexes, Chem. Eur. J. 26(16) (2020) 3479–3483. doi:10.1002/chem.201905100
- 135. H. Y. Chen, C. S. Teng, P. H. Lin, C. P. Liu, W. M. Liu, L. K. Chu, Noncovalent association thermodynamics of turnon fluorescent probes with human serum albumin: Dual-concentration ratio method, ChemBioChem 24(19) (2023) e202300370. doi:10.1002/cbic.202300370
- 136. R. Sabate, L. Rodriguez-Santiago, M. Sodupe, S. J. Saupe, S. Ventura, Thioflavin-T excimer formation upon interaction with amyloid fibers, Chem. Commun. 49 (2013) 5745–5747. doi:10.1039/C3CC42040J
- 137. A. Rybicka, G. Longhi, E. Castiglioni, S. Abbate, W. Dzwolak, V. Babenko, M. Pecul, Thioflavin T: Electronic circular dichroism and circularly polarized luminescence induced by amyloid fibrils, ChemPhysChem 17(18) (2016) 1–8. doi:10.1002/cphc.201600235
- 138. V. Gabelica, R. Maeda, T. Fujimoto, H. Yaku, T. Murashima, N. Sugimoto, D. Miyoshi, Multiple and cooperative binding of fluorescence light-up probe Thioflavin T with human telomere DNA G-quadruplex, Biochemistry 52(33) (2013) 5620–5628. doi:10.1021/bi4006072
- 139. C. P. M. van Mierlo, H. H. J. de Jongh, A. J. W. G. Visser, Circular dichroism of proteins in solution and at interfaces, Appl. Spectrosc. Rev. 35(4) (2000) 277–313. doi:10.1081/ASR-100101227
- 140. J. M. Khan, A. Ahmed, S. F. Alamery, O. H. A. Alghamdi, S. Azmi, A. Malik, Perturbation of anionic surfactant induced amyloid fibrillation by chemical chaperone: A biophysical study, J. Mol. Liq. 315 (2020) 113717. doi:10.1016/j.molliq.2020.113717
- 141. N. Berova, L. Di Bari, G. Pescitelli, Application of electronic circular dichroism in configurational and conformational analysis of organic compounds, Chem. Soc. Rev. 36 (2007) 914–931. doi:10.1039/B515476F
- 142. G. P. Spada, Alignment by the convective and vortex flow of achiral self-assembled fibers induces strong circular dichroism effects, Angew. Chem. Int. Ed. 47(4) (2008) 636–638. doi:10.1002/anie.200704602
- 143. M. Wolffs, S. J. George, Z. Tomovic, S. C. J. Meskers, A. P. H. J. Schenning, E. W. Meijer, Macroscopic origin of circular dichroism effects by alignment of self-assembled fibers in solution, Angew. Chem. 46(43) (2007) 8203–8205. doi:10.1002/ange.200703075
- 144. J. Kardos, M. P. Nyiri, E. Moussong, F. Wien, T. Molnár, N. Murvai, V. Tóth, H. Vadászi, J. Kun, F. Jamme, A. Micsonai, Guide to the structural characterization of protein aggregates and amyloid fibrils by CD spectroscopy, Protein Sci. 34(3) (2025) e70066. doi:10.1002/pro.70066
- 145. E. D. Sitsanidis, C. C. Piras, B. D. Alexander, G. Siligardi, T. Javorfi, A. J. Hall, A. A. Edwards, Circular dichroism studies of low molecular weight hydrogelators: The use of SRCD and addressing practical issues, Chirality 30(6) (2018) 708–718. doi:10.1002/chir.22850
- 146. A. Loksztejn, W. Dzwolak, Vortex-induced formation of insulin amyloid superstructures probed by time-lapse atomic force microscopy and circular dichroism spectroscopy, J. Mol. Biol. 395(3) (2010) 643–655. doi:10.1016/j.jmb.2009.10.065
- 147. N. Berova, K. Nakanishi, R. W. Woody, (Eds.). Circular Dichroism: Principles and Applications, 2nd ed.; Wiley-VCH: New York, 2000.
- 148. N. Berova, P. L. Polavarapu, K. Nakanishi, R. W. Woody (Eds.), Comprehensive chiroptical spectroscopy, Vol. 1 and 2, John Wiley & Sons, Hoboken, New Jersey, USA, 2012.

- 149. S. Zhu, M. Sun, Electronic circular dichroism and Raman optical activity: Principle and applications, Appl. Spectrosc. Rev. 56(7) (2021) 553–587. doi:10.1080/05704928.2020.1831523
- 150. K. Harata, H. Uedaira, The circular dichroism spectra of the β-cyclodextrin complex with naphthalene derivatives, Bull. Chem. Soc. Jpn. 48(2) (1975) 375–378. doi:10.1246/bcsj.48.375
- 151. M. Kodaka, A general rule for circular dichroism induced by a chiral macrocycle, J. Am. Chem. Soc. 115(9) (1993) 3702–3705. doi:10.1021/ja00062a040
- 152. I. Matei, L. Soare, C. Tablet, M. Hillebrand, Characterization of simvastatin and its cyclodextrin inclusion complexes by absorption and circular dichroism spectroscopies and molecular mechanics calculations, Rev. Roum. Chim. 54(2) (2009) 133–141.
- 153. C. Retna Raj, R. Ramaraj, γ-Cyclodextrin induced intermolecular excimer formation of thioflavin T, Chem. Phys. Lett. 273(3–4) (1997) 285–290. doi:10.1016/S0009-2614(97)00600-3
- 154. P. K. Singh, S. Murudkar, A. K. Mora, S. Nath, Ultrafast torsional dynamics of Thioflavin-T in an anionic cyclodextrin cavity, J. Photochem. Photobiol. A Chem. 298 (2015) 40–48. doi:10.1016/j.jphotochem.2014.10.007
- 155. N. H. Mudliar, P. K. Singh, Fluorescent H-aggregates hosted by a charged cyclodextrin cavity, Chem. Eur. J. 22(22) (2016) 7394–7398. doi:10.1002/chem.201600925
- 156. A. M. Pettiwala, P. K. Singh, Supramolecular dye aggregate assembly enables ratiometric detection and discrimination of lysine and arginine in aqueous solution, ACS Omega 2(12) (2017) 8779–8787. doi:10.1021/acsomega.7b01546
- 157. M. Kasha, H. R. Rawls, M. Ashraf El-Bayoumi, The exciton model in molecular spectroscopy, Pure Appl. Chem. 11(3–4) (1965) 371–392. doi:10.1351/pac196511030371
- 158. N. Harada, S. M. L. Chen, K. Nakanishi, Quantitative definition of exciton chirality and the distant effect in the exciton chirality method, J. Am. Chem. Soc. 97(19) (1975) 5345–5352. doi:10.1021/ja00852a005
- 159. N. Harada, A. G. Petrovic, N. Berova, Spectroscopic analysis: Exciton circular dichroism for chiral analysis, Comprehensive Chirality 8 (2012) 449–477. doi:10.1016/B978-0-08-095167-6.00846-6
- 160. M. Groenning, Binding mode of Thioflavin T and other molecular probes in the context of amyloid fibrils—current status, J. Chem. Biol. 3 (2010) 1–18. doi:10.1007/s12154-009-0027-5
- 161. V. Babenko, T. Harada, H. Yagi, Y. Goto, R. Kuroda, W. Dzwolak, Chiral superstructures of insulin amyloid fibrils, Chirality 23(8) (2011) 638–646. doi:10.1002/chir.20996
- 162. A. Loksztejn, W. Dzwolak, Chiral bifurcation in aggregating insulin: An induced circular dichroism study, J. Mol. Biol. 379(1) (2008) 9–16. doi:10.1016/j.jmb.2008.03.057
- 163. A. Fulara, W. Dzwolak, Bifurcated hydrogen bonds stabilize fibrils of poly(L-glutamic) acid, J. Phys. Chem. B 114(24) (2010) 8278–8283. doi:10.1021/jp102440n
- 164. G. V. De Ferrari, W. D. Mallender, N. C. Inestrosa, T. L. Rosenberry, Thioflavin T is a fluorescent probe of the acetylcholinesterase peripheral site that reveals conformational interactions between the peripheral and acylation sites, J. Biol. Chem. 276(26) (2001) 23282. doi:10.1074/jbc.M009596200
- 165. N. R. Rovnyagina, N. N. Sluchanko, T. N. Tikhonova, V. V. Fadeev, A. Yu. Litskevich, A. A. Maskevich, E. A. Shirshin, Binding of thioflavin T by albumins: An underestimated role of protein oligomeric heterogeneity, Int. J. Biol. Macromol. 108 (2018) 284–290. doi:10.1016/j.ijbiomac.2017.12.002
- 166. J. Kumar, T. Nakashima, T. Kawai, Circularly polarized luminescence in chiral molecules and supramolecular assemblies, J. Phys. Chem. Lett. 6(17) (2015) 3445–3452. doi:10.1021/acs.jpclett.5b01452

- 167. R. Sabaté, U. Baxa, L. Benkemoun, N. Sánchez de Groot, B. Coulary-Salin, M. Maddelein, L. Malato, S. Ventura, A. C. Steven, S. J. Saupe, Prion and non-prion amyloids of the HET-s prion forming domain, J. Mol. Biol. 370(4) (2007) 768–783. doi:10.1016/j.jmb.2007.05.014
- 168. C. Ritter, M. L. Maddelein, A. B. Siemer, T. Luhrs, M. Ernst, B. H. Meier, S. J. Saupe, R. Riek, Correlation of structure and infectivity of the HET-s prion, Nature 435 (2005) 844–848. doi:10.1038/nature03793
- 169. C. Wasmer, A. Lange, H. Van Melckebeke, A. B. Siemer, R. Riek, B. H. Meier, Amyloid fibrils of the HET-s(218-289) prion form a beta solenoid with a triangular hydrophobic core, Science 319(5869) (2008) 1523–1526. doi:10.1126/science.1151839
- 170. R. Khurana, C. Coleman, C. Ionescu-Zanetti, S. A. Carter, V. Krishna, R. K. Grover, R. Roy, S. Singh, Mechanism of thioflavin T binding to amyloid fibrils, J. Struct. Biol. 151(3) (2005) 229–238. doi:10.1016/j.jsb.2005.06.006
- 171. M. Groenning, L. Olsen, M. van de Weert, J. M. Flink, S. Frokjaer, F. S. Jorgensen, Study on the binding of Thioflavin T to beta-sheet-rich and non-beta-sheet cavities, J. Struct. Biol. 158(3) (2007) 358–369. doi:10.1016/j.jsb.2006.12.010
- 172. M. Groenning, M. Norrman, J. M. Flink, M. van de Weert, J. T. Bukrinsky, G. Schluckebier, S. Frokjaer, Binding mode of Thioflavin T in insulin amyloid fibrils, J. Struct. Biol. 159(3) (2007) 483–497. doi:10.1016/j.jsb.2007.06.004
- 173. L. Qin, J. Vastl, J. Gao, Highly sensitive amyloid detection enabled by thioflavin T dimers, Mol. BioSyst. 6 (2010) 1791–1795. doi:10.1039/C005255H
- 174. C. C. Kitts, D. A. Vanden Bout, Near-field scanning optical microscopy measurements of fluorescent molecular probes binding to insulin amyloid fibrils, J. Phys. Chem. B 113(35) (2009) 12090–12095. doi:10.1021/jp903509u
- 175. M. Biancalana, K. Makabe, A. Koide, S. Koide, Molecular mechanism of thioflavin-T binding to the surface of β-rich peptide self-assemblies, J. Mol. Biol. 385(4) (2009) 1052–1063. doi:10.1016/j.jmb.2008.11.006
- 176. Y. Miura, S. Namioka, A. Iwai, N. Yoshida, H. Konno, Y. Sohma, M. Kanai, K. Makabe, Redesign of a thioflavin-T-binding protein with a flat β -sheet to evaluate a thioflavin-T-derived photocatalyst with enhanced affinity, Int. J. Biol. Macromol. 269(1) (2024) 131992. doi:10.1016/j.ijbiomac.2024.131992
- 177. F. Zsila, E. Hazai, L. Sawyer, Binding of the pepper alkaloid piperine to bovine β -lactoglobulin: circular dichroism spectroscopy and molecular modeling study, J. Agric. Food Chem. 53(26) (2005) 10179–10185. doi:10.1021/jf051944g
- 178. L. Di Bari, S. Ripoli, P. Salvadori, Serum albumin and natural products, in Progress in Biological Chirality, G. Palyi, C. Zucchi and L. Caglioti (Eds.), 2004, Elsevier Ltd, pp. 271–295. doi:10.1016/B978-008044396-6/50025-3
- 179. S. Bais, P. K. Singh, Al³+-Responsive ratiometric fluorescent sensor for creatinine detection: Thioflavin-T and sulfated-β-cyclodextrin synergy, ACS Appl. Bio Mater. 6(10) (2023) 4146–4157. doi:10.1021/acsabm.3c00349
- 180. D. N. de Vasconcelos, V. F. Ximenes, Albumin-induced circular dichroism in Congo red: Applications for studies of amyloid-like fibril aggregates and binding sites, Spectrochim. Acta A Mol. Biomol. Spectrosc. 150 (2015) 321–330. doi:10.1016/j.saa.2015.05.089
- 181. N. H. Mudliar, P. K. Singh, Emissive H-aggregates of an ultrafast molecular rotor: A promising platform for sensing heparin, ACS Appl. Mater. Interfaces 8(46) (2016) 31505–31509. doi:10.1021/acsami.6b12729
- 182. A. A. Maskevich, A. V. Lavysh, I. M. Kuznetsova, A. I. Sulatskaya, K. K. Turoverov, Spectral manifestations of aggregation of the molecules thioflavin T, J. Appl. Spectrosc. 82 (2015) 33–39. doi:10.1007/s10812-015-0060-9

- 183. A. V. Lavysh, A. A. Lugovskii, E. S. Voropay, A. I. Sulatskaya, I. M. Kuznetsova, K. K. Turoverov, A. A. Maskevich, Aggregation of thioflavin T and its new derivative in the presence of anionic polyelectrolyte, Biointerf. Res. Appl. Chem. 6(5) (2016) 1525–1530.
- 184. A. M. Pettiwala, P. K. Singh, A molecular rotor based ratiometric sensor for basic amino acids, Spectrochim. Acta A Mol. Biomol. Spectrosc. 188 (2018) 120–126. doi:10.1016/j.saa.2017.06.035
- 185. D. Fedunova, P. Huba, J. Bagelova, M. Antalik, Polyanion induced circular dichroism of Thioflavin T, Gen. Physiol. Biophys. 32(2) (2013) 215–219. doi:10.4149/gpb_2013020
- 186. S. P. Pandey, A. A. Awasthi, P. K. Singh, Supramolecular tuning of thioflavin-T aggregation hosted by polystyrene sulfonate, Phys. Chem. Chem. Phys. 23 (2021) 14716–14724. doi:10.1039/d1cp02030g
- 187. G. Ionita, S. Mocanu, I. Matei, Conformational preferences of TEMPO type radicals in complexes with cyclodextrins revealed by a combination of EPR spectroscopy, induced circular dichroism and molecular modeling, Phys. Chem. Chem. Phys. 22 (2020) 12154–12165. doi:10.1039/D0CP01937B
- 188. A. Biancardi, T. Biver, A. Burgalassi, M. Mattonai, F. Secco, M. Venturini, Mechanistic aspects of thioflavin-T self-aggregation and DNA binding: evidence for dimer attack on DNA grooves, Phys. Chem. Chem. Phys. 16 (2014) 20061–20072. doi:10.1039/c4cp02838d
- 189. S. Murudkar, A. K. Mora, S. Jakka, P. K. Singh, S. Nath, Ultrafast molecular rotor based DNA sensor: An insight into the mode of interaction, J. Photochem. Photobiol. A Chem. 295 (2014) 17–25. doi:10.1016/j.jphotochem.2014.08.012
- 190. Y. Xue, H. Xie, Y. Wang, S. Feng, J. Sun, J. Huang, X. Yang, Novel and sensitive electrochemical/fluorescent dual-mode biosensing platform based on the cascaded cyclic amplification of enzyme-free DDSA and functional nucleic acids, Biosens. Bioelectron. 218 (2022) 114762. doi:10.1016/j.bios.2022.114762
- 191. B. Zhang, T. Zhu, L. Liu, L. Yuan, In vitro electrochemical detection of the degradation of amyloid-β oligomers, J. Coll. Interf. Sci. 629(B) (2023) 156–165. doi:10.1016/j.jcis.2022.09.009
- 192. N. Alsiraey, H. D. Dewald, Nitroxidative stress in human neural progenitor cells: In situ measurement of nitric oxide/peroxynitrite imbalance using metalloporphyrin nanosensors, J. Inorg. Biochem. 263 (2025) 112785. doi:10.1016/j.jinorgbio.2024.112785
- 193. M. A. Mihai, T. Spataru, S. Somacescu, O. G. Moga, L. Preda, M. Florea, A. Kuncser, N. Spataru, Nitrite anodic oxidation at Ni(ii)/Ni(iii)-decorated mesoporous SnO₂ and its analytical applications, Analyst 148 (2023) 6028–6035. doi:10.1039/D3AN01249B
- 194. F. Branzoi, M. A. Mihai, S. Petrescu, Corrosion protection efficacy of the electrodeposit of poly (n-methyl pyrrole-Tween20/3-methylthiophene) coatings on carbon steel in acid medium, Coatings 12(8) (2022) 1062. doi:10.3390/coatings12081062
- 195. A. J. Veloso, V. W. S. Hung, G. Sindhu, A. Constantinof, K. Kerman, Electrochemical oxidation of benzothiazole dyes for monitoring amyloid formation related to the Alzheimer's disease, Anal. Chem. 81(22) (2009) 9410–9415. doi:10.1021/ac901940a
- 196. V. Dounin, A. Constantinof, H. Schulze, T. T. Bachmann, K. Kerman, Electrochemical detection of interaction between Thioflavin T and acetylcholinesterase, Analyst 136 (2011) 1234–1238. doi:10.1039/C0AN00743A
- 197. B. O. Okesola, Y. Wu, B. Derkus, S. Gani, D. Wu, D. Knani, D. K. Smith, D. J. Adams, A. Mata, Supramolecular self-assembly to control structural and biological properties of multicomponent hydrogels, Chem. Mater. 31(19) (2019) 7883–7897. doi:10.1021/acs.chemmater.9b01882
- 198. G. A. Balan, A. Precupas, I. Matei, Gelation behaviour of pluronic F127/polysaccharide systems revealed via thioflavin T fluorescence, Gels 9(12) (2023) 939. doi:10.3390/gels9120939

- 199. C. Ota, T. Konishi, S. I. Tanaka, K. Takano, Induced circular dichroism analysis of thermally induced conformational changes on protein binding sites under a crowding environment, Chemphyschem 25(1) (2024) e202300593. doi:10.1002/cphc.202300593
- 200. L. de Carvalho Bertozo, M. Kogut, M. Maszota-Zieleniak, S. A. Samsonov, V. F. Ximenes, Induced circular dichroism as a tool to monitor the displacement of ligands between albumins, Spectrochim. Acta A Mol. Biomol. Spectrosc. 278 (2022) 121374. doi:10.1016/j.saa.2022.121374
- 201. K. J. Y. Low, A. Venkatraman, J. S. Mehta, K. Pervushin, Molecular mechanisms of amyloid disaggregation, J. Adv. Res. 36 (2022) 113–132. doi:10.1016/j.jare.2021.05.007
- 202. C. Wells, S. Brennan, M. Keon, L. Ooi, The role of amyloid oligomers in neurodegenerative pathologies, Int. J. Biol. Macromol. 181 (2021) 582–604. doi:10.1016/j.ijbiomac.2021.03.113
- 203. T. Kaku, K. Ikebukuro, K. Tsukakoshi, Structure of cytotoxic amyloid oligomers generated during disaggregation, J. Biochem. 175(6) (2024) 575–585. doi:10.1093/jb/mvae023
- 204. S. D. Choudhury, J. Mohanty, H. P. Upadhyaya, A. C. Bhasikuttan, H. Pal, Photophysical studies on the noncovalent interaction of thioflavin T with cucurbit[n]uril macrocycles, J. Phys. Chem. B 113(7) (2009) 1891–1898. doi:10.1021/jp8103062
- 205. J. Mohanty, S. D. Choudhury, P. Upadhyaya, A. C. Bhasikuttan, H. Pal, Control of the supramolecular excimer formation of thioflavin T within a cucurbit[8]uril host: A fluorescence on/off mechanism, Chem. Eur. J. 15(21) (2009) 5215–5219. doi:10.1002/chem.200802686
- 206. S. Murudkar, A. K. Mora, P. K. Singh, T. Bandyopadhyay, S. Nath, An ultrafast molecular rotor based ternary complex in a nanocavity: a potential "turn on" fluorescence sensor for the hydrocarbon chain, Phys. Chem. Chem. Phys. 17 (2015) 5691–5703. doi:10.1039/c4cp04636f
- 207. A. Biancardi, T. Biver, B. Mennucci, Fluorescent dyes in the context of DNA-binding: The case of Thioflavin T, Int. J. Quantum Chem 117(8) (2017) e25349. doi:10.1002/qua.25349
- 208. C. Wu, Z. Wang, H. Lei, Y. Duan, M. T. Bowers, J. E. Shea, The binding of Thioflavin-T and its neutral analog BTA-1 to protofibrils of the Alzheimer Aβ16-22 peptide probed by molecular dynamics simulations, J. Mol. Biol. 384(3) (2008) 718–729. doi:10.1016/j.jmb.2008.09.062
- 209. L. S. Wolfe, M. F. Calabrese, A. Nath, D. V. Blaho, A. D. Miranker, Y. Xiong, Protein-induced photophysical changes to the amyloid indicator dye thioflavin T, Proc. Natl. Acad. Sci. U. S. A. 107(39) (2010) 16863–16868. doi:10.1073/pnas.1002867107
- 210. T. Wang, L. H. Zeng, D. L. Li, A review on the methods for correcting the fluorescence inner-filter effect of fluorescence spectrum, Appl. Spectrosc. Rev. 52(10) (2017) 883–908. doi:10.1080/05704928.2017.1345758
- 211. C. Wu, M. Biancalana, S. Koide, J. E. Shea, Binding modes of thioflavin-T to the single-layer β -sheet of the peptide self-assembly mimics, J. Mol. Biol. 394(4) (2009) 627–633. doi:10.1016/j.jmb.2009.09.056
- 212. S. K. Mudedla, N. A. Murugan, H. Ågren, Effect of familial mutations on the interconversion of α-Helix to β-sheet structures in an amyloid-forming peptide: insight from umbrella sampling simulations, ACS Chem. Neurosci. 10(3) (2019) 1347–1354. doi:10.1021/acschemneuro.8b00425
- 213. M. Harel, L. K. Sonoda, I. Silman, J. L. Sussman, T. L. Rosenberry, Crystal structure of thioflavin T bound to the peripheral site of Torpedo californica acetylcholinesterase reveals how thioflavin T acts as a sensitive fluorescent reporter of ligand binding to the acylation site, J. Am. Chem. Soc. 130(25) (2008) 7856–7861. doi:10.1021/ja7109822
- 214. A. Rybicka, M. Pecul, Induced circular dichroism of thioflavin T interacting with acetylcholinesterase: A computational study, Chem. Phys. 463 (2015) 82–87. doi:10.1016/j.chemphys.2015.10.005

215. H. Ren, B. P. Fingerhut, S. Mukamel, Time resolved photoelectron spectroscopy of thioflavin T photoisomerization: A simulation study, J. Phys. Chem. A 117(29) (2013) 6096–6104. doi:10.1021/jp400044t